CFD ANALYSIS FOR THE DETERMINATION OF DISCHARGE COEFFICIENT BY USING A PRISMATIC SILL BELOW A VERTICAL SLUICE GATE

A DISSERTATION

SUBMITTED IN PARTIAL FULFILLMENT OF REQUIREMENTS

FOR THE AWARD OF A DEGREE OF

MASTER OF TECHNOLOGY

IN

HYDRAULICS AND WATER RESOURCES ENGINEERING

Submitted by

NIMAN KOSAR ALI

(2K20/HFE/08)

Under the Guidance of

Dr. BHARAT JHAMNANI

(ASSISTANT PROFESSOR)

DEPARTMENT OF CIVIL ENGINEERING

DELHI TECHNOLOGICAL UNIVERSITY

(Formerly Delhi College of Engineering)

Bawana Road, Delhi-110042

May 2022

DELHI TECHNOLOGICAL UNIVERSITY

(Formerly Delhi College of Engineering)

Bawana Road, Delhi-110042

CANDIDATE DECLARATION

I, Niman Kosar Ali, Roll. No. 2K20/HFE/08, an M.Tech. in Hydraulics and Water Resources Engineering student, hereby declare that the project dissertation titled **"CFD Analysis for The Determination of Discharge Coefficient by Using a Prismatic sill Below a Vertical Sluice Gate,"** which I submitted to the Department of Civil Engineering, Delhi Technological University, in partial fulfillment of the requirement for the award of a degree of "Master of Technology the best of my knowledge, no one else has submitted this research work embodied in the thesis for the award of any degree, diploma, or certificate.

Place**:** Delhi

Date: May 2022

Niman kosar Ali

2k20/HFE/08

DELHI TECHNOLOGICAL UNIVERSITY

(Formerly Delhi College of Engineering)

Bawana Road, Delhi-110042

CERTIFICATE

I hereby certify that the Project Dissertation titled "**CFD Analysis for The Determination of Discharge Coefficient by Using a Prismatic sill Below a Vertical sluice Gate**" submitted by, Roll number **2K20/HFE/08**, Department of Civil Engineering, Delhi Technological University in partial fulfillment of the requirement for the award of a Master of Technology degree is a record of the project work carried out by the students under my supervision. To the best of my knowledge, this work has never been submitted for a degree or diploma at this university or anywhere else.

Place: Delhi **Dr. BHARAT JHAMNANI**

Date: May 2022 (**SUPERVISOR)**

ABSTRACT

Sluice gates are commonly used to control water flow through irrigation canals. Free flow or submerged flow occurs when the flow is dependent on the upstream head, gate opening, and downstream head. Once the sluice gate depth is higher than certain layout criteria, the use of double or triple leaf gates is common. The goal of this research is to see how constructing a sill with a well-defined form below a sluice gate alters the flow submerged underneath. In comparison to other downstream slopes of sills, studies have shown that the sill of the trapezoidal with a downstream slope of 1Vertical and 5Horizontal enhances discharge under the gate which generates the smallest increase in the length of jump developed through the downstream section. It is taken into account both subcritical and supercritical flow. The main consideration for the flow below the sluice gate was the discharge coefficient of the sluice gate. The simulations are run on a CFD-based software with a Flume of the proper length and sills of various heights under a variety of flow conditions. The coefficient of discharge was correlated to the other relevant flow and sill variables using dimensional analysis. The discharge coefficient predictions obtained using the developed equations are compared. H/G the head-gate opening ratio difference, H1/G Ratio of upstream head-gate openings, z/b characteristics of the sill, and Yt/G tail-water depth-gate having opened ratio all influence the discharge coefficient. It was discovered that for submerged subcritical flow, the tempo of change of the discharge of coefficient is higher and moderate for critical submerged flow, and for the submerged supercritical flow, the rate of change is mostly constant.

ACKNOWLEDGEMENT

I'd like to express my heartfelt gratitude to my supervisor **Dr. Bharat Jhamnani**, who provided me with the wonderful opportunity to complete this project on the topic "**CFD Analysis for The Determination of Discharge Coefficient by Using a Prismatic sill Below a Vertical Sluice Gate**," which also assisted me in conducting extensive research and learning about many new things. and I have greatly benefited from his vast knowledge. I extend my gratitude to my college, Delhi Technological University (Formerly Delhi College of Engineering) for allowing me to carry out this project. This opportunity will be a significant milestone in my career development. I will strive to use the gained skills and knowledge in the best possible way, and I will continue to work on their improvement, to attain desired my career objectives.

Place**:** Delhi **Niman Kosar Ali**

Date: May 2022 2k20/HFE/08

Table of Contents

LIST OF FIGURES

LIST OF TABLES

ABREVATIONS

A - sill cross-section area.

Cd -- Coefficient of discharge.

G -- Gate opening.

g --- Acceleration due to gravity.

H ---- Upstream flow depth above the flume bed.

HI --- Upstream flow depth above the sill crest.

P --- Sill wetted perimeter.

q --- Discharge per unit width.

R_s --- Discharge per unit width.

Z ---- sill height.

CHAPTER 1:
INTRODUCTION

1.1 Background

Sluice gates are without a doubt one of the most useful and significant controller and metric devices. The sluice gate's discharge of coefficient is determined by geometric and hydraulic variables. Sluice gates are regarded among the most essential flow through regulator controllers. Sluice gates are classified into two groups based on the downstream water level: free flow and submerged flow. Because of the significance of the sluice gate as a control device in hydraulic engineering, numerous researchers have looked into the prediction of flow characteristics via gates in the past. When the height of the sluice gate exceeds certain design criteria, double or triple leaf gates are provided as needed. Sluice gates are hydraulic components which are used to measure the flow rate and way of measuring outflow rate in various channels. Depend on the depth of the water downstream of the gate to the gate opening, this entrance can be free or sunken. They are suitable for use in prismatic or non-prismatic channels. Mostly every water resource project includes a reservoir or diversion project to regulate flooding or hold water for irrigation or electricity production, as well as a domestic or industrial supply of water. During extreme flood inflows, a spillway with a proper stopping mechanism is usually supplied for the discharge of water. Control devices installed in passageways in the dam's body and tunnels can also be used to release water. A gate or shutter is available to measure the flow of water by placing a leaf or a closure member across the waterway from an external position. Valves control the flow in closed pipes, such as penstocks carrying water for hydropower, and differ from gates in that they come with the driving tools, so although gates demand a different drive or hoisting instrument.

Because flow occurs in open channels due to energy differences, the proper operation of the gate is critical. Upstream depth corresponds to flow Y1 and downstream depth corresponds to flow Y2, and a vertical sluice gate is provided for flow control. Different types of gates are available for specific purposes, and they can be installed in various locations and operated with appropriate hoists. A brief overview of the most common types of valves used to regulate flow in penstocks is also provided.

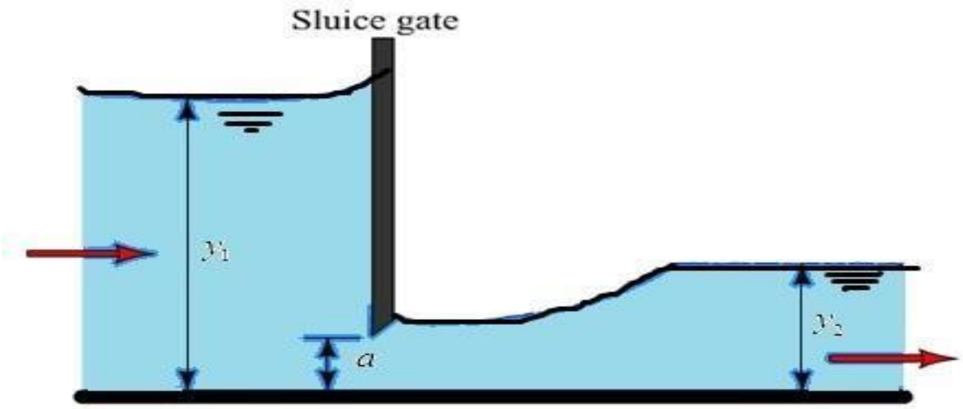

Figure 1. 1:flow below a vertical sluice gate

The Bureau of Indian Standards code IS 13623: 1993 "Requirements for choice of gates and hoists" provides the basic classification of gates, which can be done through using following criteria.

1) Sluice gate location about reservoir water surface basis
2) Head of water over gate sill basis
3) The Operational requirement basis
4) Fabrication material basis
5) Basis of operation mode
6) The shape of the gate
7) Discharge through gate basis
8) The kind of and position of the fluid flow to which it is attached to Seal position basis
9) Skin plate location basis
10) Closing characteristics basis
11) Drive to operate basis

1.2 Gates are divided into several categories.

1.2.1 Based on the location of the opening of the potable headwater

Crest or Surface gates, which are designed to close overflowing water,
or Deep-seated or Submerged gates,

which are submerged on both sides during implementation, are the two types of gates used in water resource works. The following are the various types of gates that fall into these categories:

Gates of the crested type include

a) vertical gates
b) radial gates
c) sector gates
d) ring gates
e) stony gates
f) falling gates
g) two-tiered entrances, and
h) Dropping Shutters

Deep-seated gates include the following:

a) a vertical gate.
b) a radial gate with a spacious seat
c) A disc-shaped gate
d) Cylindrical gates are the fourth type of gate.
e) Follow the gate ring behind you.
f) For a jet, a flow gate
g) Gate with a seal ring

1.3 Sluice gate needed requirement

near the plant walls, water-resistant surfaces corrosive waste liquid resistance, ensuring long-term service life simple design with few parts required for installation and maintenance no skewing or jamming of the gate no great effort required to move the gate A relatively low metal capacity ensures reliability.

1.3.1 Factors to be considered when choosing sluice gate

1. Geological condition
2. Water flow conditions
3. Construction and management conditions

1.3.2 The type and location of the flow passage to which it is connected

Gates are used to opening the majority of the openings in any water resource project. Spillways, sluices, intakes, regulators, pipework, passageways, and other structures, to name a few, can all be used to control flow. The following list divides gates into categories based on their connection to a specific waterway. The hydropower gates have only been sketched out here in a rudimentary form. It's listed below.

1. The gate of the penstock
2. Sluice gate
3. Surge shaft gate
4. Construction of a sluice gate
5. the gate of the head regulator
6. For balancing gates
7. The gates of the crest
8. Depletion sluice gate
9. Locked gate for navigation
10. Tunnel diversion gate no.

1.3.3 Based on Sill's head

1. A low headgate is one with a head of fewer than 15meters.
2. A medium headgate is one with a head between 15 and 30 meters
3. A high headgate is one with a head height of more than 30 meters.

1.3.4 Based on operational requirements

a) Access entrance (main gate): Used mostly for flow regulation and routine procedures, such as the entrance for spillway sluices and outlets.

b) Emergency closure gates, such as an emergency penstock gate, are used to close an opening in flowing water in the event of an emergency.

c) Access entrance: Bulkhead gates, urgent gates, and stop-logs are all used to maintain service gates.

Construction gates, such as building sluice gates and diversion tunnel gates, are needed to close an opening during building works or to completely close it after construction.

1.3.5 Based on the fabrication material

a) Gates made wooden doors
b) Gates made with aluminum
c) Gates made of fabric (plastic) or rubber
d) Made-of-cast-iron gates
e) Concrete-reinforced gates
f) Steel doors.

1.3.6 Mathematical Model

The actual discharge to its theoretical value is well known as the coefficient of discharge Cd which simulates the physical properties of the flow phenomena including flow losses, defined as

$$q = cd * G\sqrt{2g(H-Z)} \quad \textbf{(1)}$$

The discharge per unit width is marked by **q.**

The upstream flow depth just above channel bed is symbolized by H.

G signifies the gate opening, Z the height of the sill well above bed, g the gravitational acceleration, and Cd the discharge coefficient.

$$Q_{th} = G*W\sqrt{2g\Delta H} \quad \textbf{(2)}$$

Q_{th} = theoretical discharge passing through the gate opening

G = gate opening provided

W = width of channel

ΔH = head difference available

The ratio of actual discharge to theoretical discharge is the value of the discharge coefficient. $Cd = \frac{Q_{act}}{Q_{th}}$ **(3)**

Cds, the discharge of a submerged silled sluice gate, can be proven as follows:

$$C_{ds} = \Psi\left[F_G, \frac{H_1}{G}, \frac{Y_t}{G}, \frac{\Delta H}{G}, \frac{Z}{B}, \frac{Z}{b}\right] \quad \textbf{(4)}$$

The flowing equation could be used to determine the coefficient of discharge (Cds) of a sluice gate with sill for submerged flow:

The flowing equation could be used to determine the coefficient of discharge (Cds) of a sluice gate with sill for submerged flow:

$$C_{ds} = \frac{Q}{GW\sqrt{2g(H_1 - H_2)}} \qquad \textbf{(5)}$$

In which W is the width of the flume

1.3.7 Significance of Froude Number

The scientist William Froude inspired the number Froude. It is determined by the speed-to-length ratio. It resembles the Mach number in some ways. It is not usually regarded in theoretical fluid dynamics because in the case of a negligible external field, the formulas are usually regarded in the high Froude limit.

The Froude number is a significant figure in naval architecture, which is used to calculate the resistance of a partially submerged moving object through water. In open channel flows, the ratio of flow velocity to the square root of the product of gravity acceleration and hydraulic gradient. The dimensionless quantity in dimension assessment is an amount that has no physical dimensions. The product or ratio of the quantities with dimensions is used to define these dimensionless quantities. Strain is a unit of measurement for deformation that can be written as the ratio of change in length to the initial length. A strain has no dimensions because the unit is 'L' in both cases.

The prototype models are evaluated using dimensionless numbers. Reynolds numbers, Weber's number, and Froude's number are the three numbers. The Froude number governs dynamic similarity in situations where the gravitational force is significant. Flow-through open channels, flow over the dam's spillway, and so on.

The ratio of inertia force to gravity force is important in open channel flow. In general, the Froude number depends on the depth of the water to classify flow as subcritical or supercritical. When a flow transitions from supercritical flow ($Fr > 1$) to subcritical flow (Fr 1), or from risky flow to the strongest flow, it is said to be a hydraulic jump. The values of Reynolds number and Weber number are unaffected by the turbulent flow generated and the surface tension value is ignored. The following relationship can be used to represent the Froude number.

$$\mathrm{Fr} = \frac{\mathrm{V}}{(\mathrm{gy})^{0.5}}$$

The depth of flow is expressed by 'y,' the acceleration due to gravity is symbolised by 'g,' and the celerity or gravity of the small surface wave is indicated by 'v.'

1.4 Open channel classifications

Open channel hydraulic structures are a topic of a lot of curiosity to civil engineers and are concerned with the flows of a free surface in channels built for supplying irrigation, water, drainage, and generating hydroelectric power in partially filled sewers, culverts, and tunnels, as well as in natural streams and rivers. An unobstructed path is a passageway with a free surface on which liquid flows. On the other hand, pipe flow occurs when the fluid fills the pipe and water flow under pressure. The pipe flow pipe is caused by a difference in pressure (gradient of pressure), whereas an open channel's flow is induced by the channel bed's incline (i.e., as a result of gravity). It's worth noting that the flow contained within a closed conduit isn't always the same as the flow through a pipe. When a liquid has a free surface, it is necessary to classify it as a flow of the open channels.

There are many different kinds of open channels. Open channels are divided into two types based on the cross-section type: Prismatic Channels and Non-Prismatic Channels. Prismatic channels have a steady bottom slope and a persistent cross-section all across their length. Over other forms, prismatic channels can be triangular, rectangular, parabolic, trapezoidal, or circular. Artificial channels commonly use prismatic channels.

The cross-section of a non-prismatic channel is non-uniform, and the bottom slope differs. The majority of natural channels are non-prismatic.

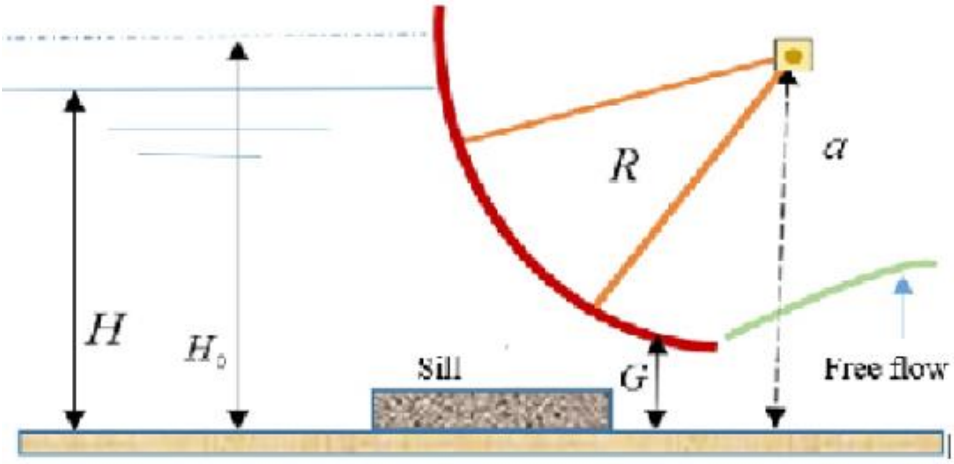

Figure 1. 2: gate with rectangular sill

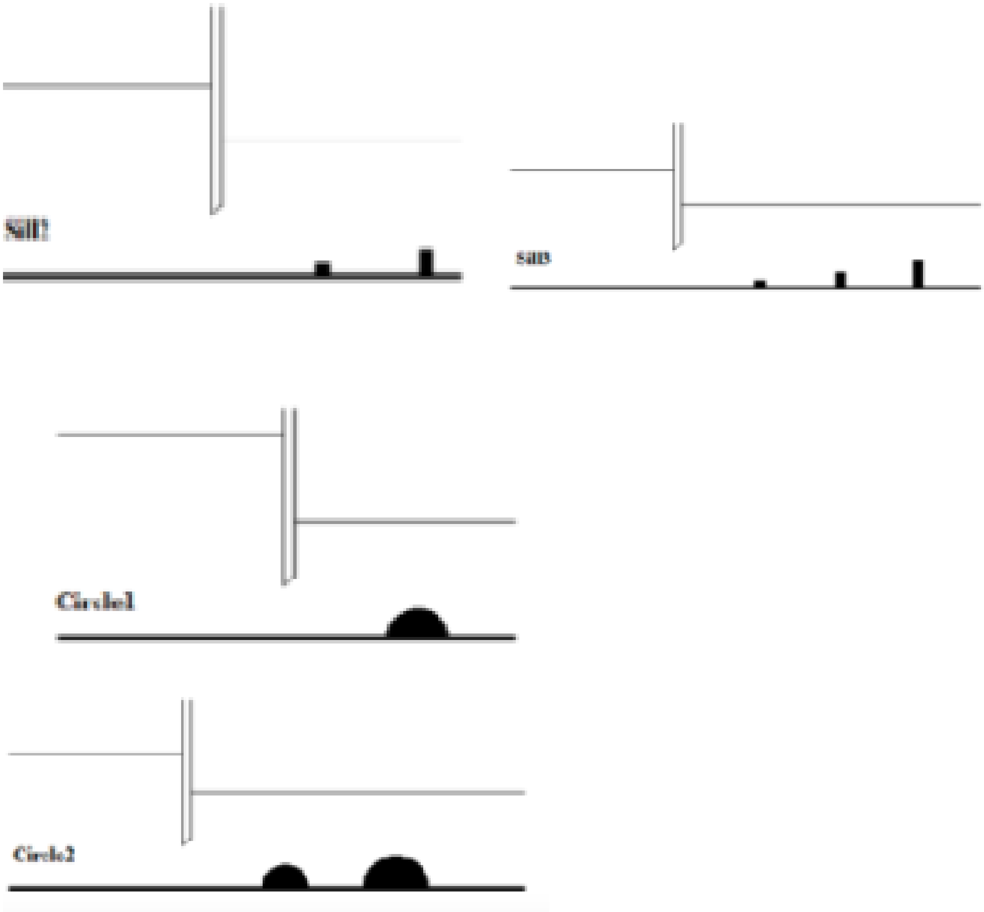

Figure 1. 3: sluice gate with circular sills

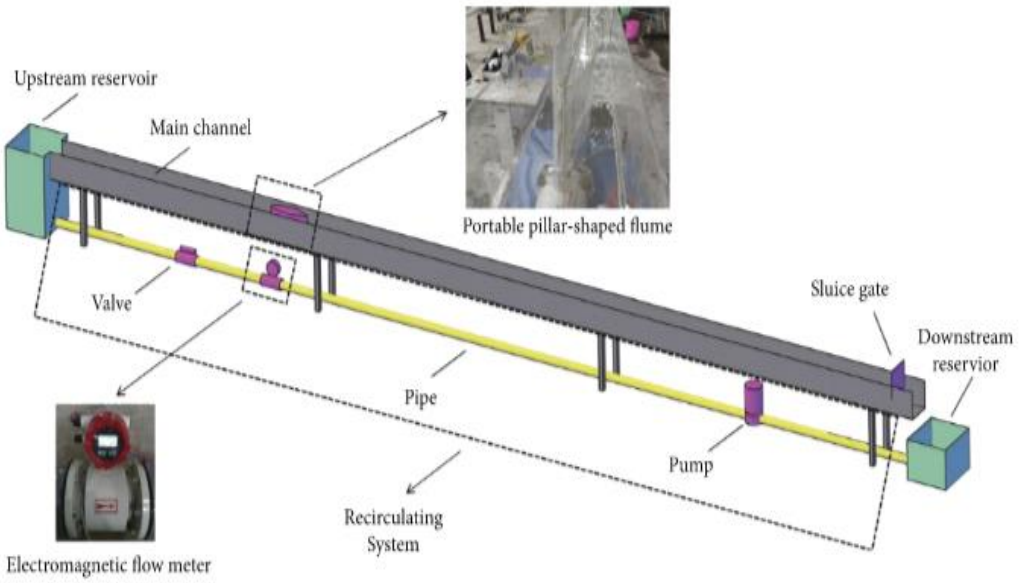

Figure 1. 4: vertical sluice gate in flume

1.5 Computational fluid dynamics (CFD)

Fluid Dynamics Computational CFD, or computational fluid dynamics, is the mathematical modelling and numerical solution of a physical phenomenon encompassing fluid flow. When an engineer is given the task with developing a new product, such as a championship-winning race car for the coming season, aerodynamics plays an important role in the design phase. During in the conceptual phase, however, aerodynamic processes are hard to quantify. An engineer only implies of optimising his designs is to undertake physical tests on product designs. Fluid Dynamics by Computation (CFD) has become a prevalent tool to create fluid flow solutions that include or exclude solid interaction as computers became more powerful and computational power has enhanced. Fluid flow is evaluated utilising CFD software in terms of physical properties like velocity, pressure, temperature, density, and viscosity. Those properties must be considered when developing a virtual solution for a physical phenomenon comprising fluid flow. A CFD software tool for analysing fluid flow employs a numerical method and a mathematical model of the physical case.

For example, the Navier-Stokes (N-S) equations are used to demonstrate the mathematical model of the physical case. This includes changes in all of those physical properties for both fluid flow and heat transfer. A mathematical model's content varies based on the problem at hand, such as heat transfer, mass transfer, phase change, chemical reaction, and so on. Furthermore, the accuracy of a CFD analysis is highly dependent on the overall structure of the process. To generate an accurate case for solving the issue, the mathematical model must be verified. Establishing accurate mathematical methods is also necessary for generating an accurate outcome. Thermal Conduction (Diffusion) is the transfer of heat from high to low temperatures across materials such as solids or fluids.

The transport of heat through the flow of a fluid is known as thermal convection. External work (forced convection) or buoyancy (the movement of varying density fluids in the presence of gravity) can drive fluid flow.

The generation and absorption of heat via electromagnetic waves are referred to as thermal radiation.

Transitions such as boiling, melting, condensation, and others release or absorb heat.

Compressible and incompressible flows: When compressibility becomes a significant factor, this type of analysis aids in the rapid and accurate discovery of solutions. A Large Eddy Simulation of flow around a cylinder is one example.

Laminar and turbulent flows: Various turbulence models are used in this sort of investigation. Turbulence simulations and their intricate numerical models necessitate a significant amount of computing power. The most difficult aspect of turbulence simulation is the simulation of changes over time. The entire domain where the simulation occurs must be recalculated at each time step. A valve could be designed using a turbulent flow assessment. Use of computational fluid dynamics.

- Design based on simulation rather than "build and test"
- Computational fluid dynamics (CFD) produces a high-fidelity database for analyzing flow fields and has a more cost-effective way and faster than EFD.
- Simulation of difficult-to-experiment physical fluid occurrences

1.5.1 Fluid properties and flow conditions in physics

1. Inviscid, viscous, laminar, turbulent, and so on are some of the flow fluid characteristics.

2. Density, viscosity, and thermal conductivity are just a few examples of fluid flow properties.

3. In industrial commercial CFD software, Flow conditions and characteristics are typically displayed in three dimensions, whereas non-dimensional variables are used in research codes. Model selection: various models are mostly fixed by a system of codes, with the user being able to select Appropriate boundary Conditions. The user must specify the Initial and Boundary Conditions for each implementation because they are not fixed by codes.

1.5.2 Post-processing using analysis and Visualization methods

1. Derivative variable calculation Vorticity
2. Shear stress on the wall
3. Integral parameter calculations: forces, moments

The use of visualization (with commercial software mostly)

4. Contours in two dimensions are simple.
5. 5.3D contour isosurface plot lines
6. Vector plots and streamlines are two examples of vector plot lines (Lines whose tangent direction is the same as the velocity vectors are called streamlines).
7. And in animations.

1.5.3 Modelling details include the following:

1. Geometry and domain
2. Coordinate systems
3. Equations in theory
4. The flow domain
5. Conditions for starting and stopping
6. Model selection for a variety of uses

1.5.4 Modelling governing equations

1.Equations of Navier-Stokes (3D in Cartesian coordinates)

2.Convection

3. Pressure gradient by piezometry

4.Terms with a high viscosity

5.Local

6.Continuity formula

7.Rayleigh Equation

8. state equation.

1.6 CFD Process

CFD is a method of applying the techniques of one discipline (numerical analysis) to another (fluid flow/mass transfer and heat transfer). Why not use an experimental approach instead of CFD because it is more reliable, such as wind tunnel experiments. Many engineering problems cannot be solved through the use of an analytical or experimental approach, or are difficult to solve using an analytical or experimental approach.

Theoretical approach: This method provides an accurate solution, which is a significant benefit. However, analytical solutions are only possible for a small number of issues, which are generally articulated in an idealized, artificial manner.

Experimental approach: These methods are dependable and depict real-life scenarios. Wind Tunnel experiments, for example, are extremely reliable in the aerospace industry. However, these can be quite costly, and they can even have some technical glitches, it can take several years to set up an experiment and resolve all technical problems.

1.6.1 Methods of computational fluid dynamics

1. Finite element method: A numerical technique for solving partial differential equations (PDEs) is the finite element method (FEM). The first and most important feature is that the continuum field, or domain, is divided into cells, or elements, that form a grid. The elements in 2D can be rectilinear or curved and have a triangular or quadrilateral shape. It is not necessary to structure the grid. Complex shapes can be handled with convenience using unstructured grids and curved cells. The finite difference method (FDM), which requires a structured grid, but which can be curved, does not have this important advantage. The finite volume method (FVM) has the same geometric flexibility as the finite element method (FEM).

2.The finite volume method (FVM) is a method of describing and analyzing partial differential equations based on algebraic equations. In the finite volume method, the divergence theorem is being used to incorporate volume integrals in a partial differential equation that contains a divergence term to surface integrals.

3. Finite difference method: The method uses dimensional operator partitioning to produce one-dimensional advection-diffusion formulae. The first-order derivatives are then estimated using upstream-type difference approximations, whereas the second-order derivatives are guesstimated using non-standard difference approximations. This approach enhances the numerical solutions' conduct substantially in terms of quality.

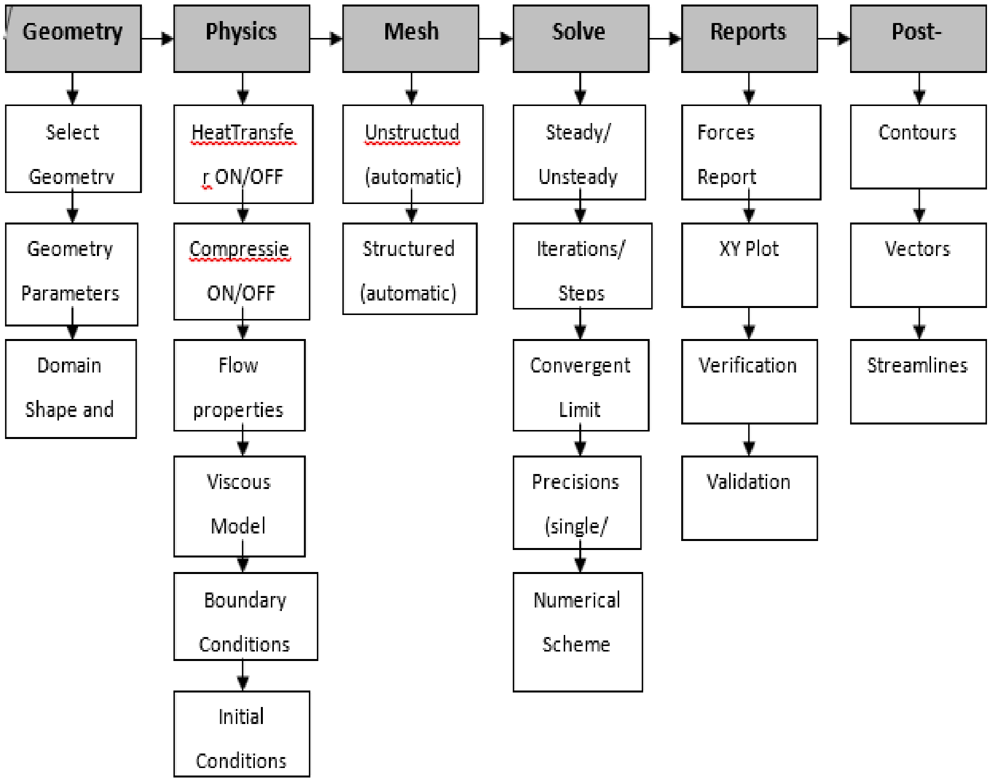

Figure 1. 5: CFD process

1.7 ANSYS FLUENT

Ansys is a developer of engineering simulation software (computer-aided engineering,) based on proprietary computational fluid dynamics (CFD) program, which is one of its most important products. One of the most widely used commercial Computational fluid dynamics software packages is Ansys fluent. The Finite Volume Method is used in the Ansys fluent computational fluid dynamics Solver.

The domain is discretized into a finite number of control amounts. On this set of control quantities, general conservation equations for mass, energy, momentum, species, and so on are solved. Ansys fluent procedure steps are mentioned below

1. Pre-analysis
2. Geometry creation
3. Meshing
4. Physics setup
5. solutions based on numbers
6. Validation and verification

1.7.1 ANSYS WORKBENCH

Ansys workbench is a Graphical User Interface that allows users to access easily all of the necessary tools and software from a single location. Ansys workbench includes tools for pre-processing, post-processing, and solving items. Workbench will allow you to manage your workflow smoothly across multiple tools.

Pre-Analysis: Using Ansys fluent to numerically overcome a real-world engineering problem. This necessitates the use of boundary conditions. to either perceive or collect data to represent the actual situation we can also obtain related theoretical or experimental results from previous studies to correlate with your Ansys simulation results. Those steps are difficult and require more attention, especially when it comes to obtaining the proper boundary conditions to achieve satisfactory results that apply to the actual case.

Geometry: The geometry must be created. Ansys design modeler software, which we can get from Ansys workbench, can be used for this. On the other hand, we can use any Cad software to create geometry, such as Autocad, Solid Works, Catia, Autocad Inventor, and so on.

Meshing: One of the most crucial steps in your simulation is meshing. Mesh quality has a significant impact on simulation results. Poor mesh quality can lead to poor simulation results, including divergence.

A mathematical model of a physical system that includes a part or assembly, properties of the material, and boundary conditions is known as finite element analysis (FEA). Simple hand calculations cannot precisely try to estimate product behaviour in several situations.

FEA is a basic method for accurately capturing physical phenomena utilising partial differential equations to represent complex behaviours. FEA has advanced to the point where both design engineers and specialists can use it. One of the most key steps in running a precise FEA simulation is meshing. A mesh is made up of many parts that represent the shape of the geometry and have nodes (space coordinates that vary by element type). Irregular shapes are challenging for a FEA solver to collaborate with, but common forms like cubes are simpler. The method of converting irregular shapes into more easily recognizable volumes known as "elements" is known as meshing.

Physics setup: It is carried out with the Ansys solver. Physics setup, numerical results, and Verification & Validation of the outputs of the solution. providing inputs for solution precision, boundary condition, physics inputs, material needed, and associated properties, among other things, during the physics setup step. In a nutshell, you use this tool to numerically represent the real-world scenario you want to simulate.

Boundary condition: Boundary conditions include flow inlets and exits, wall, repeating, pole, and internal face boundaries, to mention a few. Commonly used boundary condition types.

Velocity Inlet: These are suitable for incompressible flow compared to compressible flow.

Unless a user-defined function is used, it seems to perform a uniform velocity profile at the boundary.

Pressure Outlet: It can handle incompressible and compressible flows. The static gauge pressure of the component through which the flow exists is the input here.

Wall Boundaries: It functions similarly to a physical barrier. At the walls of viscous flow, slip conditions will not be applied. Wall roughness can be defined as turbulent flows.

Solution Methods: It's crucial to choose the right method for solving the problem you want. Every method has their own set of advantages and disadvantages. For pressure and momentum, we can also select a discretization method. Second-order schemes produce more precise results, while first-order schemes aid in convergence.

A popular method is the coupled method, which aids in convergence. If we get divergence in the simple method for any simulation, we can try the Coupled method, which can sometimes solve the divergence problem.

1.8 Methods for predicting turbulent flows

Direct numerical simulation (DNS) Is a method for solving the Navier-Stokes equations for all of the motions in a turbulent flow. This method is "exact" because all turbulence scales are solved, but it places a high demand on computational resources. DNS is currently only possible for geometries with low Reynolds numbers and simple geometries. It's used to research and understand turbulence, as well as to verify RANS and LES turbulence models.

Large-eddy simulation. (LES) This method is used to filter the Navier-Stokes equations. This implies that only the tiniest turbulent eddies are excluded (those smaller than a filter's mesh size, Large-scale motions in the flow are solved, while small-scale motions are modelled. To accomplish closure, the filtering process brings new unknown parameters that must be modelled. Here, as well, turbulence models are used. Because they're only used to model turbulence on scales smaller than the filter's grid size, they're called subgrid-scale models. Computation accuracy can be improved, but at the expense of extra computer requirements, since this method helps solve more turbulence and models less (in contrast to RANS).

Reynolds averaged Navier-Stokes (RANS) The Navier-Stokes equations are averaged to get these equations (time-averaging if the flow is statistically steady or ensemble-averaging for time-dependent flows). Only the mean flow is solved with the RANS equations, while all turbulence scales must be modeled (i.e., approximated). Because the averaging process introduces new unknowns (Reynolds stresses), the RANS equations do not form a closed set. As a result, approximations must be made. Turbulence models (e.g., k-models) are these approximations. In the field of numerical computation of wind flow around buildings and airflow inside buildings, the RANS method is the most widely used and validated.

1.8.1 Need for the Proposed Study

Irrigation projects consist of canal systems and structure works to regulate the flow in the system. Sluice Gates are used to controlling the discharge and water level. Sills below sluice gates reduce their height and weight, especially in cross regulators constructed in deep channels.

We are determining the value of Coefficient of discharge (C_d) with relating data of actual discharge (Qact) and (Q_{th}) done with previous experimental research works which are validated with Numerical Simulation through ANSYS Software.

The major criterion for the flow underneath the sluice gate is the discharge coefficient of the sluice gate.

1.9 Objectives

(1) To identify the effect of upstream head-on discharge coefficient by providing a trapezoidal sill.

(2) To see how the height of the sill affected the discharge coefficient.

(3) To identify the effect of subcritical and supercritical flow.

(4) To investigate the effect of dimensionless parameters like z/b, z/B, and H_1/G.

CHAPTER 2:

LITERATURE REVIEW

Abbott and Kline (1962) discovered asymmetric flow patterns on an expansion transition during their experiments. They also discovered that the flow pattern is unaffected by Reynolds numbers or turbulence intensities.

Young (1982) investigated the concept of a stepped sill, which evolved from a stepping spillway. By use of a stepped spillway for the topmost still, the water dam reduced energy consumption by 75%. He successfully dissipates the energy by adding so many stages to the downstream side of the spillway, and the deflecting flow jet is removed. Along with him, Sorensen experimented on a physical model of a stepped spillway, discovering to add a few stages to the downstream edge from the hydraulic spillway to remove the deflecting flow of jet.

Panda (1981) and Tanwar (1984) found that the Froude number, the ratio of flow depth to side sluice gate opening, and the ratio of tailwater depth to side floodgate opening all influence the coefficient of discharge of side sluice gates.

Sorensen (1985) Conducted an actual model exploration for stepped sill and observed that introducing a few segments to the spillway face removed the differing water jet.

Salem (1990) examines the impact of an upper flat sill and an upper curved sill located below a radial entrance of different elevations under various flow scenarios.

It was observed that when used with a radial entrance, the upper curved sill enhanced the Cd by almost 12% more than just the flat top sill.

Saiad et al. (1991) used trapezoidal flat top sills carried out for different slopes and heights to show the impact of a sill under the gate for underwater fluid properties. Increasing the downstream slope of the sill increases the discharge coefficient, according to his research. Ibrahim and his colleagues also looked at data from supercritical submerged flows with a fixed Froude number Fr in their experiments (1.806, 1.462, 1.255, and 1.018). He discovered that when the lateral sill is built at a range of 34 of the watershed length from the entrance, the coefficient of discharge reaches its peak value.

The coefficient of discharge in a sluice gate is a complex feature of geometric modes and hydraulic variables, **Swamee, (1992)** It is attributed to the depth of upstream and entrance gate for free flow, and it is related to tail-water depth for immersed flow in moreover to these parameters. The current way of determining discharge coefficient is to draw curves connecting the coefficient of discharge and depth of upstream gate-opening ratio, with the rear gate-opening ratio as the third variable for underwater flow. Because of the correlation of two different types of curves, this technique lends itself to an adequate amount of error. In his research, he developed important discharge coefficient formulas for free and immersed flows, in addition to a set of standards for determining free and submerged flow. There are also techniques for solving various gate-opening issues.

Samir (1994) compared the flow characteristics of a jump under a submerged gate by using physical and numerical simulation models. Around 20 tests were performed to check how the spacing between the corrugated beds influenced basic functions. These corrugated beds reduce the length of the jump and successive depth by an average of 5.69% and 12.96 percent.

Press, (1995), Flood routing in prismatic channels has been solved using free surface flow equations. The kinetic energy variables are developed into a partial differential equation with two aspects related to the cross-sectional area and discharge of the prismatic channels in this new formulation. An explicit finite difference system was used to solve these equations. Going to follow the estimation of the discharge using the new conservation equations, the correlating cross-sectional area was calculated using the continuity equation.

Broeck (1997) used numerical simulations to evaluate the free surface flow just below a sluice gate and showed that the assumption of a uniform flow upstream was incorrect.

Negm and Alhamid (1998) studied the impacts of constructing a known-form sill beneath a sluice gate on the immersed flow beneath it. Analyses have shown that the trapezoidal sill with a downstream slope of 1V:5H enhances discharge below the gate and generates the fewest increase in the jump length formed downstream when particularly in comparison to other downstream slopes of sills**.** As a result, the data collected from experiments on the downstream slope's under-gate sill will be analyzed. It is taken into account both subcritical and supercritical flow.

The main criterion for the flow below the gate was the discharge coefficient of the gate. The tests were carried out on a small laboratory flume, with sills of various heights being tested under a variety of flow conditions. The discharge coefficient was correlated to the other relevant flow and sill parameters using dimensional analysis. Using nonlinear regression analysis, dimensionless general equations in terms of flow and sill parameters are developed for determining the discharge coefficient of the gate (sluice) with the sill. The discharge coefficient predictions obtained utilizing the constructed formulas are contrasted to the experiment values. The constructed formulas have demonstrated high accuracy and reliability.

Negm et al. (1998) examined the impact of sill parameters Z/b and Z/B (Z= height of sill, b= the sill's upper width, B= lower width of the sill) on the flow below a submerged gate with a sill. With his research, discovered that the sill below the entrance increases the discharge coefficient of the entrance, and the rate of increase is dependent on the configuration of both the sill and the gate, as well as the sill and flow parameters.

Roth and Hager (1999) studied the impacts of viscosity and surface tension on the flow underneath a sluice gate and revealed two side vortices owing to stagnation flow upstream of the gate.

Alhamid, (1999) examined the free gate flow regime, and the influence of the shape of the sill beneath the sluice gates on the discharge coefficient was explored. Also, the height and shape of the sill are both investigated. Polygonal and non-polygonal sills were among the shapes evaluated. The most efficient of the shapes tested are circular sills, and triangular sills are the best of the polygonal sills. In addition to its shape, the height of the sill has a significant impact on the coefficient of discharge. Utilizing non-linear regression analysis and dimensional analysis, for both silled and non-silled cd free gate flows, the discharge coefficient was forecast. Flow variables, gate opening, sill height, and sill shape variables were all factored into the equation.

Swamee et al. (Rajaratnam (2000) offered an equation for calculating the coefficient of discharge in free flow using the dimensionless parameter y=a and in submerged flow using the factors y=a and yt=a.

Negm, A.M. et al. (2001) studied the behavior of underwater flow under a vertical gate with a sill upstream of a horizontal varying stream, of a lab flume of ten cm wide, 31 cm in-depth, and 3.0 meters in length, The availability of a sill under the gate has a major impact on the gate's coefficient of discharge, and the feature detection in the discharge coefficients is dependent on the Froude number below the gate and the differential head proportion.

Chanson (2002) discovered a fascinating subset of the three systems. The presence or absence of hydraulic structures on the stair bed is used to divide the chin flow regime into the following sub. The skimming flow regime is segmented based on the path geometry and flow conditions, leading to various flow field configurations close to the steps.

Ghodsian, (2003) studied the subject of research. Experimentally, the hydraulic properties of the gate's side were investigated. The specific energy of the side of the gate was discovered to be constant. The flow from the sided sluice gates determines the Froude number of the major channel and the ratio depth of upstream of flow to sluice entrance opening to allow for free flow. One other major factor that influences is the proportion of water tail depth to flow submerged gate entrance. The released coefficient equations were found to be appropriate.

Debabeche & Achour,(2007) These findings were put to the test in a 90-degree central angle horizontal symmetrical triangular channel. This aims to investigate the essential qualities of both the minimum width jump and the controlled-sill jump under the different inflow instances. To speed up the continuation of jumps, a thin-crested or broad-crested sill has been used. The data were subjected to correlation coefficients to determine the effect of the inflow Froude number on comparative sill apex, eventual depths ratio, and non-dimensional sill toe position Based on a large-scale test program. The gained interactions should be used to design irrigation systems.

Kim, (2007) The contraction and discharge coefficients, as well as for free movement past a sluice gate, the pressure distribution, can be calculated using numerical tools based on the Reynolds averaging Navier-Stokes equations. Experimental studies have shown that the established inviscid theoretical contractility coefficient has a very large variation.

If the entrance opening rate becomes less than 0.4, the contractility coefficient decreases as the gate opening rate rises, and tends to increase when the lock opening rate is greater than 0.4m, displaying a trend when compared to previous experimental measurements This is due to increased energy losses due to friction and surface of water oscillations as approach velocity from the gate rises and opening gate rate surpasses 0.4m.

Saad (2007) examines the impact of circular crested sill forms on supercritical smooth flow under floodgates. The Cd value is affected by the geometric pattern of the sill; however, the curvature of the sill has no influence mostly on hydraulic jump components.

Lozano et al., (2009) investigates the Canal irrigation scheme in Lebrija, Spain, approximately 16,000 field-measured statistics areas were used to calibrate four rectangular gates for immersed-flow conditions. At each of the gate structures, acoustic sensors were used to measure the depth of water and gate opening values, and the information was recorded on electronic data loggers. The rectangular sluice gates were found to be capable of accurate flow measurement when a variety of gate measurement equations were put to the test The E-M equations (Energy-Momentum) were found to be valid. For three of the four gates studied, the adjustment of the coefficient of construction, which was used in the formula of energy, resulted in accurate discharge estimations. The entrance for which the E-M technique did not undertake well at the canal's mouth, with a one-of-a-kind nonsymmetric flow pattern. In addition, he looked into the effectiveness of the traditional flow equation. The relationship between the flow coefficient of discharge, Cd, and the head variation, h, and the opening of the vertical doorway, w, leads to the conclusion that as a function of these two parameters, Cd should be displayed. The best empirical fit for the sluice gates studied in this research was obtained by showing that Cd as a parabolic function of w, with an exponential expression previously checked by other authors, also produced average results. The calculated Cd had the most uncertainty among the variables which was explored, it is also useful to assess the ambiguity in the approximated discharge through a measured sluice gate using the uncertainty analysis method. The discharge uncertainty falls as gate opening rises, and it falls slightly as head differentials rise in each of the four different gates examined in this research.

Akoz et al. (2009) presented numerical and experimental outcomes for two-dimensional flow upstream of a sluice gate, validating that the k-e turbulence closure model can predict the velocity profile and free surface the best.

Belaud et al (2009) suggested an alternative conceptual way of calculating the coefficient of compression under sluice gates on flattened beds in both free and submerged scenarios. Especially for large gate openings, the contraction coefficient varied to comparative gate opening and relative submergence, especially for large gate openings.

AboulAtta et al., (2011) Studied the layout of this new shape and the experimental work of a roughened stilling basin that used T-shape roughness instead of frequent cubic roughness. In this study, the best intensity and roughness length were ascertained. T-shape roughness also helps in saving materials and minimizes jump length when compared to cubic roughness. According to the results of a sensitivity analysis, changing the length of the jump is relatively more sensitive to the change in roughness length ratio than the change in intensity.

Neveen Y. Saad (2011) determined the impact of circular-crested sills with various radii and persistent heights, as well as downstream and upstream slopes below vertical flood gates, on the coefficient of discharge was determined. In a flume measuring the length of 250cm and width of 15 cm, and a depth of 30 cm. Also discovered that the main factor influencing the coefficient of discharge is B/Z and that the crested-circular sill generates a larger discharge coefficient than the flat-crested sill only if its B/Z is equal to or less than that of the flat-crested sill.

***ª ¬ ' G ' Z '*, (2011)** In the case of supercritical flow, the existence of crested-circular sills with various radii under immersed vertical gates of sluice affects the coefficient discharges. A series of lab experiments were carried out for this purpose. The results revealed that the main factor affecting the discharge coefficient for crested-circular sills is B/Z (B= width of the bottom sill, Z= height sill). Only if the crested-circular sill's B/Z is smaller than the flat top sill's does the crested-circular sill have a higher discharge coefficient than the flat top sill. The major factor that influences the coefficient of discharge is B/Z, according to these experiments.

Only if the B/Z of the crested-circular sill is the same to or less than that of the plain-crested sill does the crested-circular sill produce a higher coefficient discharge than the plain-crested sill. Because the models with abrupt changes in crest have a smaller B/Z than the smooth crested ones, the Cd values obtained by the models with abrupt changes in the crest are higher than those obtained by the smooth crested ones with the same radii.

Hussain et al. (2011) investigated three-dimensional (3D) velocities and streamlined patterns in open channels under free-flow conditions at the centreline of sharp-crested rectangular side orifices. They observed that almost all streamlines diverge towards the orifice for flows with a low Froude number. Just those streamlines that are nearly equal to the side orifice are shifted towards the orifice in the event of increased Froude number flows.

Habibzadeh et al. (2011) developed a formula for the discharge coefficient of sluice gates in rectangular channels under orifice flow in both free and submerged conditions using a theoretical method. Under free- and submerged-flow conditions, the new equations can be used to forecast the rendition of sluice gates with different edge shapes.

Bagheri and Heidarpour (2012) studied flow velocity in three dimensions near the side weir and over the crest. The longitudinal velocity peaked near the beginning of the side weir, while the spill flow velocity peaked close to the end, according to the observed velocity distribution data. The direction of flow near the crest has been upward, but at the deepest depths, the flow direction was inverted, likely to result in a downward flow near the water surface, as per the demonstrated vertical velocity values. For a side sluice gate to function effectively, a deeper understanding of flow characteristics in the vicinity of the gate, especially as a control system, is required. The primary goal of this research is to examine the flow velocity profile in three dimensions near a sharp-crested rectangular side sluice gate. The angle of diverted flow from the main channel to the side channel was also explored.

Cassan and Belaud (2012) studied the flow upstream of a submerged gate with a large opening and discovered that the flow is mostly two-dimensional because the velocity distribution is unlikely to be affected by the low-velocity recirculating pump.

Bassam R Jurdi and Jean G Chatila (2013) investigated the hydraulics of stepped spillways with an ogee profile, assessing their effectiveness as a substitute to streamlined spillways in stepped sill research findings.

Mishra et al. (2013) conducted a study that helped refine the layout of the baffle-sluice irrigation module. Empirical evidence interactions were demonstrated to be good in modeling the discharge.

Guven et al (2013) explored the hydraulic systems of concurrent flow across cube and square berms and over a broad crested weir. Once comparing single simulations to merged modeling techniques, they noted that the coefficient of discharge rises.

J. Farhoudi and H. Khalili Shayan (2013) Investigated the energy loss of free-flow under a sluice gate. They both present an equation for calculating the energy loss factor, as well as the impact of this parameter on the discharge coefficient's accuracy.

Jean G Chatila and Bassam R Jurdi (2013) studied the hydraulics of ogee-profile stepped spillways, assessing their suitability as a smooth-back spillway option as well as their role in preventing downstream energy and hydraulic jump length. The number of steps was revealed to be the most important element in expelling flow kinetic energy and, as a consequence, shortening the downstream formation hydraulic jump. Setup of a network of canals and the types of facilities to regulate the flow of water through the system are all part of irrigation schemes**.** The streamflow and water level are governed by gates. Sills under gates decrease the height and weight of cross regulators, especially those built-in deep channels. Many researchers have looked into submerged flow characteristics under gates with sill structures.

Gumus et al. (2013) investigated the submerged hydraulic jump under the sluice gate experimentally and numerically in a previous study.

According to **Mohanta et al., (2014)**, Flooding is a complicated issue that causes effect the livelihood and economy of the region. Recreating such flows is critical for river scientists and engineers working in this area. A mathematical exploration has been performed to study various interconnected compound channel stream characteristics, such as velocity distribution, depth-averaged velocity distribution, etc. The models which are created with ANSYS – FLUENT produce relatively satisfactory results in comparison to newly performed experimental data in a controlled manner. As a result, the main goal of this study is to use the Volume of Fluid of the two-phase model and the LES the large Eddy simulation turbulence modeling to evaluate the turbulent of a non-prismatic compound channel's shape and flow conditions are forecast. Allowing sufficient development time for a uniform turbulent flow to develop the way data is collected. However, numerical simulations of compound channels with multiple hydraulic conditions are computationally expensive and complex.

Habibzadeh et al. (2014) examined flow regimes of the deflected surface jet (DSJ) and reinserting wall jet using a submerged hydraulic jump and baffle blocks (RWJ). Flows of numerous velocities, Froude numbers, and baffle block sizes have all been a consideration.

Mohanta, Naik, et al., (2014) Examined the predicting of water different surface elevations in non-prismatic compound channels using a one-dimensional technique The numerical method is then used to calculate water surface elevation in non-prismatic compound channel configurations, with good accordance between experimental and computational data. The flow distribution in a converging compound channel is investigated using a fully three-dimensional and two-phase CFD framework. The convergence condition was determined using the finite volume method with a dynamic Sub-grid-scale. To enable the free surface to deform freely with the foundational turbulence, the quantity of fluid method was used.

L. Cassan and G. Belaud (2015) completed the numerical study of sluice gates is relatively new, but it has provided an efficient method for exploring flow characteristics and improving knowledge about gate behavior. Among the anticipated outcomes, this study aims to improve the determination of the contraction coefficient.

To that end, Ansys-Fluent was used to run 2D RANS simulations with four different turbulence models. The numerical simulations were compared to experimental results and other theoretical approaches based on potential flow assumptions used to calculate the discharge coefficient and velocity distribution graphs.

Demirel (2015) used experimental and numerical methods to study turbulent flow downstream of a underwater sluice gate. The flow velocities as well as turbulence characteristics were assessed in a laboratory flume throughout the experiments. The flow structure downstream of the sluice gate was examined using a three-dimensional computational fluid dynamics (CFD) simulation. Because of the interaction of mean flow and recirculation flow downstream of the submerged sluice gate, the flow is proved to be extremely three-dimensional and unsteady. The conversed flow leads to the formation of two corner vortices, as per the three-dimensional simulated results. Secondary velocities due to free surface vortices are about 6% of the mean jet velocity at the inlet, which is substantial for riverbank erosion. In the vicinity of the submerged gate, vortex-induced free surface variations were also noted.

Gumus et al. (2016) looked at the velocity field and surface profiles of a tailwater's submerged hydraulic jump in an open channel flow. Under the same circumstances, the article especially in comparison the results of the experiment to the simulation solution. Numerous variations of standard, renormalized, implementable k-turbulence models; k-shear stress transport model; and Reynolds' stress turbulence models are being used in the CFD model. When the outcomes of the numerous turbulence models are compared, it is evident that the Reynolds stress model gives the best outcomes.

Jalil, (2017) conducted in an open channel, the effect of a stepped sill behind a literal sluice gate on submerged flow was investigated by varying the height of the step in the sill and the gate opening. The following are the results of the statistical analysis. To a certain step height, the stepped sill improves the performance of the vertical sluice gate. With increasing Fr, D/L, h/Yt, etc., the discharge coefficient rises. With increasing P/H, H/D, Y1/Y2, Yt/D, and Yt/D, the discharge coefficient decreases. Discharge Eqs. 5 and 6 are developed within the limitations of an experiment to predict the discharge with a mean percent error of 0.017 and 0.023 respectively, with A Cd ranging from 0.33 to 0.74 and a Standard Error of 0.005725.

Aydın & Ulu, (2017) Computational Fluid Dynamics (CFDs) analysis software package programs have recently gained a lot of traction in hydraulic engineering. The goal of this review was to see how various sills affect flow dynamics. The velocity contours and orders of magnitude for each sill shape were examined in this work. Taking four cross-sections from the downstream region, the velocity magnitudes are compared. The results showed that sills downstream of the channel decrease the magnitude of the velocity at each chosen site. As a result, it was determined that sills could protect the channel bottom from cavitation bubbles and scouring damage caused by high flow velocities. In this regard, the research will aid hydraulic design ideas in this zone.

Silva and Rijo (2017) used a variety of methods to estimate the flow of water. Their results demonstrate that using an energy model to calculate the flow rate below the sl ide gates for both unrestricted and submerged flow conditions provided more finesse.

Ferro (2018) used the momentum equation for free-flow conditions to calculate the stage-discharge relationship of a sharp-crested sluice gate. The theoretically inferred formula was then determined by titration utilizing experimental data from past research findings.

Salmasi et al. (2019) studied the impacts of differential sill shapes and geometric parameters in a free-flow condition, on the coefficient of discharge (CD) of radial gates. They have a massive effect on CD, according to the observations. There were also regression equations initiated.

Sunik, (2019) Has been studied A fiberglass prototype model in a horizontal channel with a sluice gate has been used in the test. Two trapezoidal baffle block models were managed to install in 3 rows and 25 cm after the gate pair, which has been used in sills of different dimensions. Water level y and velocity have been estimated throughout each running test, and the Fr no, contraction coefficient Cc, and Cd which is the coefficient of discharge were determined by calculating. The results revealed that trapezoidal baffle block prototype T2, and no sill, 2-centimeter sill, and 2.7-centimeter sill, with Froude no equal to 0.11 to 0.75, shows the best performance of preliminary Froude number modeling of Cc and Cd, with R2 equal to 0.8086 (Cc coefficient of construction and R2 equal to 0.8273 (Cd). The outcome of the result is that free-surface flow under sluice gates is critical for irrigation and drainage channel management estimation. The flow through the gate may be free or submerged, based on the depth of the tailwater.

Ali & Elhamaimi, (2020) used physical and numerical models to make a comparison of the flow parameters of a submerged jump under the gate. In twenty experimental runs for values, the influence of equal distance corrugated beds on basic characteristics

of the underwater hydraulic jump was examined. Fr numbers ranged somewhere from 1.5 to 9.5. Experiments have been performed on a smooth surface. The volume of fluid method in FLUENT Ansys software and k-epsilon and RNG k- turbulent models has been used to make simulation in the submerged jump on the spaced corrugated bed which is the finest, depending on experiment runs. To use simulation of highly transient and turbulent flow parameters, a free surface CFD numerical model was used.
Kubrak et al., (2020) Investigated the feasibility of measuring water flow rate using an irrigation sluice gate in submerged conditions. On a 1:2 scale model, hydraulic tests on sluice gate discharge capacity were performed. The measurements were created for the flow of the submerged sluice gate. Connections and nomograms have been used to simulate the model of Cd values for the tested sluice gate. It also explored the possibility of deciding the ability of the discharge modeled gate by using the established nomogram for the ability discharge of the submerged gate.

The impact of various mounting techniques on sluice gate cross-section narrowing and capacity was discussed. The calculations proved that the formulas for the submerged sluice gate could be used to estimate irrigation sluice gate flow. Without a doubt, sluice gates are one of the most vital controller and metric devices. The coefficient of discharge of a sluice gate is determined by geometric and hydraulic variables.

Elnikhely (2020) looked at the impact of various variables on flow under a vent sluice entrance beneath free flow parameters. The cause of different expansion criteria and the lateral sills on flow characteristics were tested. The findings showed that increasing the expansion ratio contributes to greater Cd values, as well as selecting the right lateral sill design for high discharge correlation coefficients.

CHAPTER 3:

MODELING AND ANALYSIS

3.1 Materials Used

This Present work is purely based on the CFD technique and for the simulation, ANSYS Fluent is used to investigate the effect of the sill below the Sluice gate. For that different sill, heights are tested to calculate the coefficient of discharge of the sluice gate. Submerged flow through vertical gate opening is subcritical flow in which the energy equation can be applied between the upstream and downstream gates. The potential energy to overcome all of the flow resistance between the two sides is the difference between the water surface levels on both sides of the gate, it has no energy loss in theory, contrary to popular belief. Wall shear, velocity contours, pressure contours, and coefficient of discharge are analyzed using ANSYS-FLUENT software after simulations the generated results compared to the experimental research which has been done earlier.

Continuity equations

$$\frac{\partial \rho}{\partial t} + \frac{\partial (\rho u)}{\partial x} + \frac{\partial (\rho v)}{\partial y} + \frac{\partial (\rho w)}{\partial z} = 0$$

Equation of state

$$p = \rho R T$$

Momentum equations

$$x\text{-component}: \quad \rho \frac{Du}{Dt} = -\frac{\partial p}{\partial x} + \frac{\partial \tau_{xx}}{\partial x} + \frac{\partial \tau_{yx}}{\partial y} + \frac{\partial \tau_{zx}}{\partial z} + \rho f_x$$

$$y\text{-component}: \quad \rho \frac{Dv}{Dt} = -\frac{\partial p}{\partial y} + \frac{\partial \tau_{xy}}{\partial x} + \frac{\partial \tau_{yy}}{\partial y} + \frac{\partial \tau_{zy}}{\partial z} + \rho f_y$$

$$z\text{-component}: \quad \rho \frac{Dw}{Dt} = -\frac{\partial p}{\partial z} + \frac{\partial \tau_{xz}}{\partial x} + \frac{\partial \tau_{yz}}{\partial y} + \frac{\partial \tau_{zz}}{\partial z} + \rho f_z$$

$$x\text{-component}: \quad \frac{\partial(\rho u)}{\partial t} + \nabla \cdot (\rho u \vec{V}) = -\frac{\partial p}{\partial x} + \frac{\partial \tau_{xx}}{\partial x} + \frac{\partial \tau_{yx}}{\partial y} + \frac{\partial \tau_{zx}}{\partial z} + \rho f_x$$

$$y\text{-component}: \quad \frac{\partial(\rho v)}{\partial t} + \nabla \cdot (\rho v \vec{V}) = -\frac{\partial p}{\partial y} + \frac{\partial \tau_{xy}}{\partial x} + \frac{\partial \tau_{yy}}{\partial y} + \frac{\partial \tau_{zy}}{\partial z} + \rho f_y$$

$$z\text{-component}: \quad \frac{\partial(\rho w)}{\partial t} + \nabla \cdot (\rho w \vec{V}) = -\frac{\partial p}{\partial z} + \frac{\partial \tau_{xz}}{\partial x} + \frac{\partial \tau_{yz}}{\partial y} + \frac{\partial \tau_{zz}}{\partial z} + \rho f_z$$

The methods for solving CFD simulation analysis are listed below.

Step 1 **Geometry:**

3-D geometry is created by Design modular which is available in ANSYS Fluent. Selection of appropriate coordinate and determination of domain and shape is important.

*Step 2 Meshing***:**

The meshing of the Unstructured type is preferred here and the size of the meshing is set to 0.01 m for better accuracy. Proper Inlet and Outlet, wall and, Bed of the flume are defined.

Step 3 Setup:

- Pressure Based solver considering the Transient time scale is used.
- Volume of Fluid Model is used for Open channel Flow.
- For viscous, the k-epsilon standard model is used for the whole investigation.
- Boundary conditions are applied to the inlet (Pressure inlet and et), outlet (pressure outlet).

Step 4 Post-processing:

Contours for Volume fraction, Pressure, Velocity, etc are plotted. Depth of downstream and upstream and discharge are precisely measured. The result is plotted against the coefficient of discharge.

3.2 Experimental Set-Up

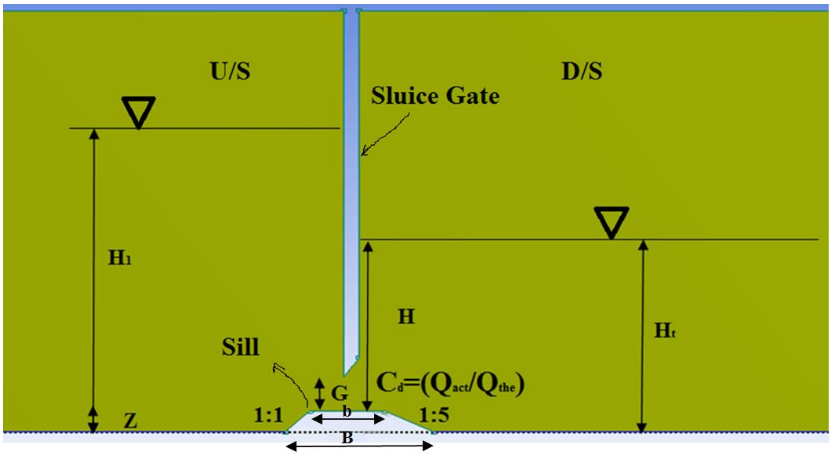

Figure 3. 1: Line diagram

The simulation is carried out using CFD on a 2.5 m long glass-sided horizontal flume. The flume bed is 10 cm wide and 20 cm deep. The water depths are evaluated using point gauges in the ANSYS Post result section of the CFD software. To control the upstream depth of the water, the flume has a sluice gate with a thickness of 5 mm plate with a tight beveled lower edge. The flume's water comes from a tank with a constant head. The tailwater is controlled by a tailgate at the flume's downstream end. Under various gate openings and discharges, trapezoidal sills of various heights **(**Z=1,2,3, and 4 cm**)** with a steady upstream slope of (1:1**)** and constant downstream slope of (1:5) are examined. Furthermore, for purposes of comparison, a flatbed model was included. The gate was located in the middle of the top width of the bellow the gate sill., which has a width of 3 cm wide. The discharge rates are various from 25 to 100 lit/min.

3.3 Models:

Gate opening ranges from 0.01 to 0.03 m to form the subcritical and supercritical flow. By increasing the velocity, the inlet, the subcritical, and supercritical flows are achieved on a fixed gate opening. And the above statement is repeated with different sill heights.

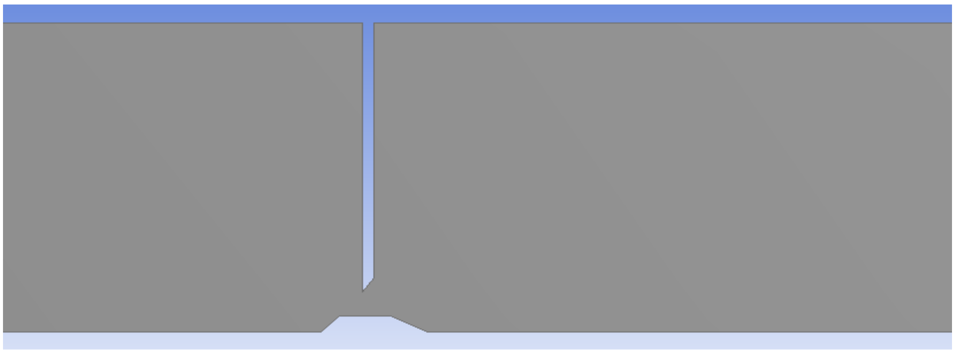

Figure 3. 2: Sill height 1 cm with Gate opening (0.01 to 0.03 m)

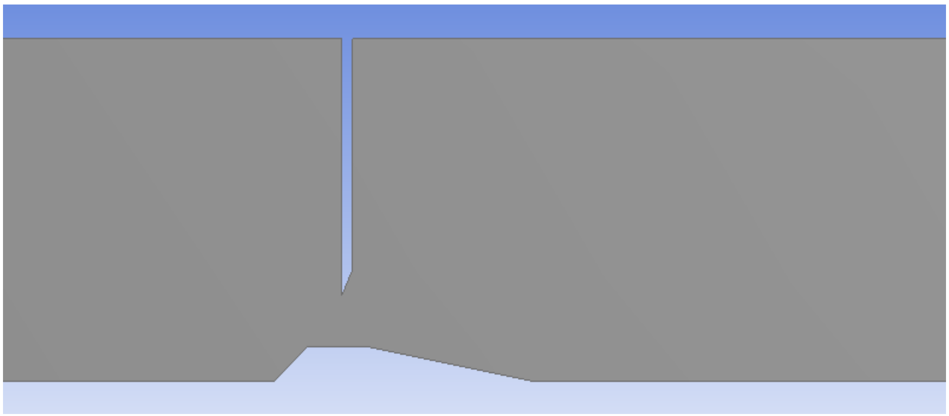

Figure 3. 3: Sill height 2cm with gate opening (0.01 to 0.03 m)

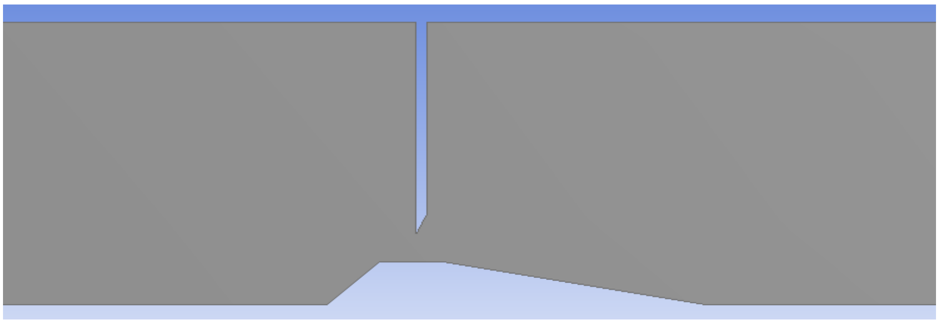

Figure 3. 4: Sill height 3cm with gate opening (0.01 to 0.03 m)

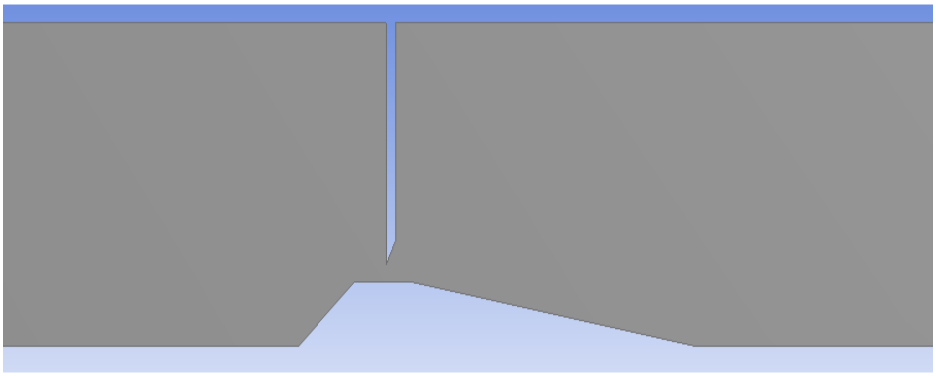

Figure 3. 5 Sill height 4 cm with gate opening (0.01 to 0.03 m)

3.4 Geometry and meshing

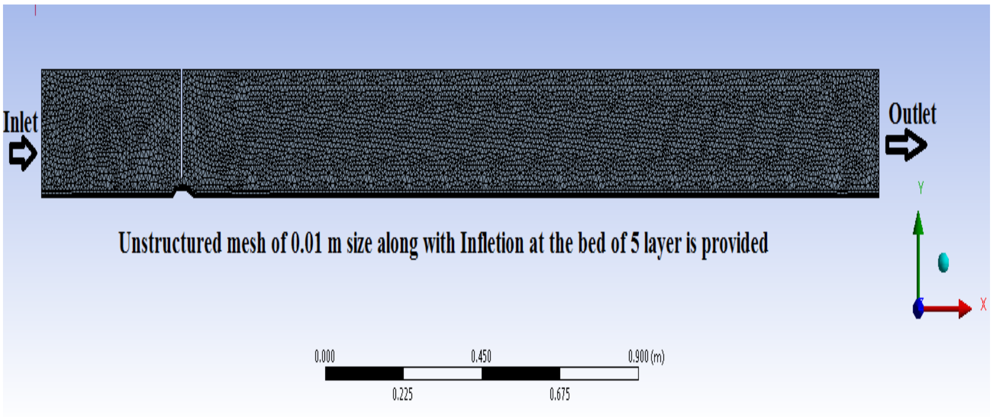

Figure 3. 6: Geometry & Meshing:

3.5 Ansys Results

3.5.1 Model 1 (SILL HEIGHT Z=1 cm)

(a) Upstream Depth is fixed at 0.15 m, and Sluice gate opening is fixed at G1

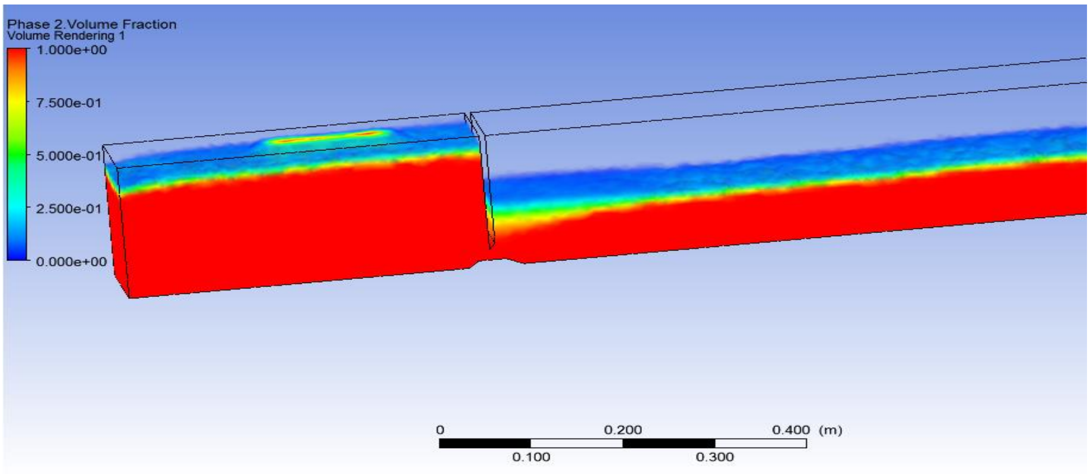

Figure 3. 7: Volume fraction

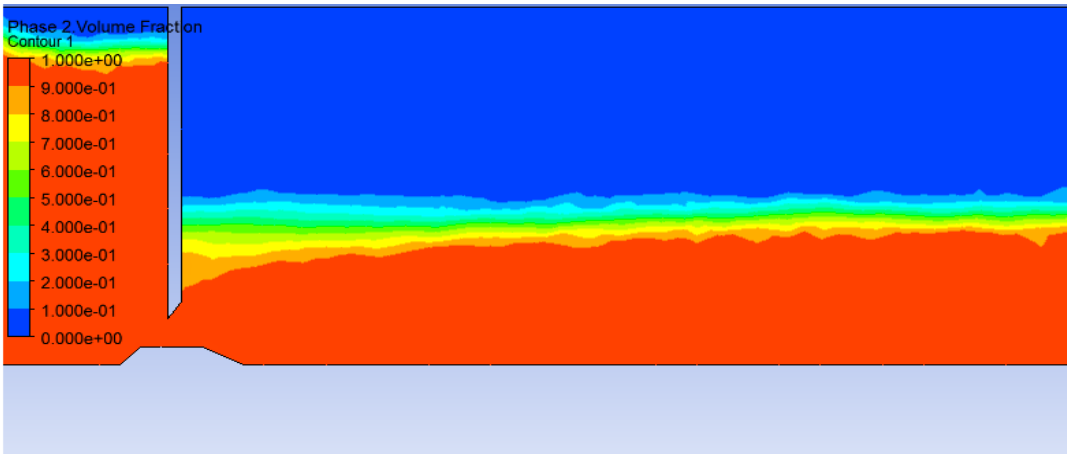

Figure 3. 8: Volume Contour:

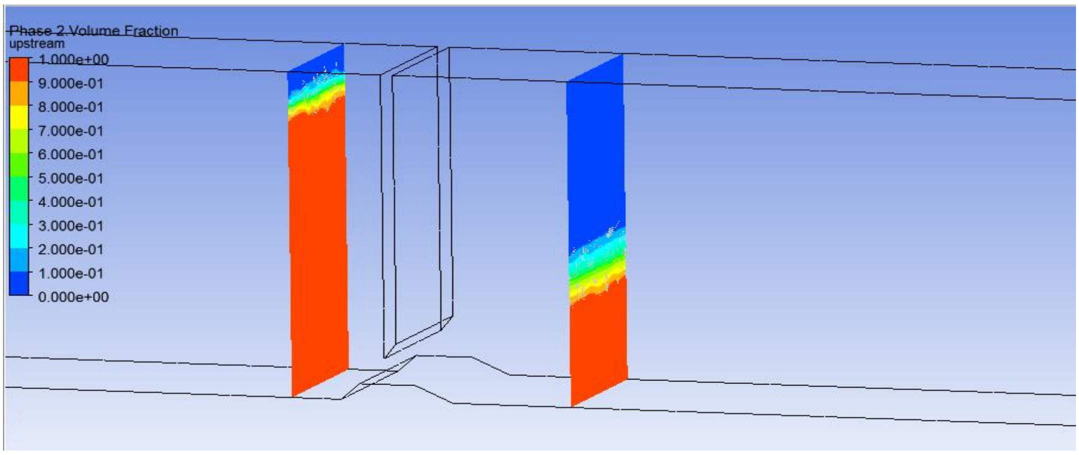

Figure 3. 9: Depth of water in the flume Upstream and Downstream of Sluice gate.

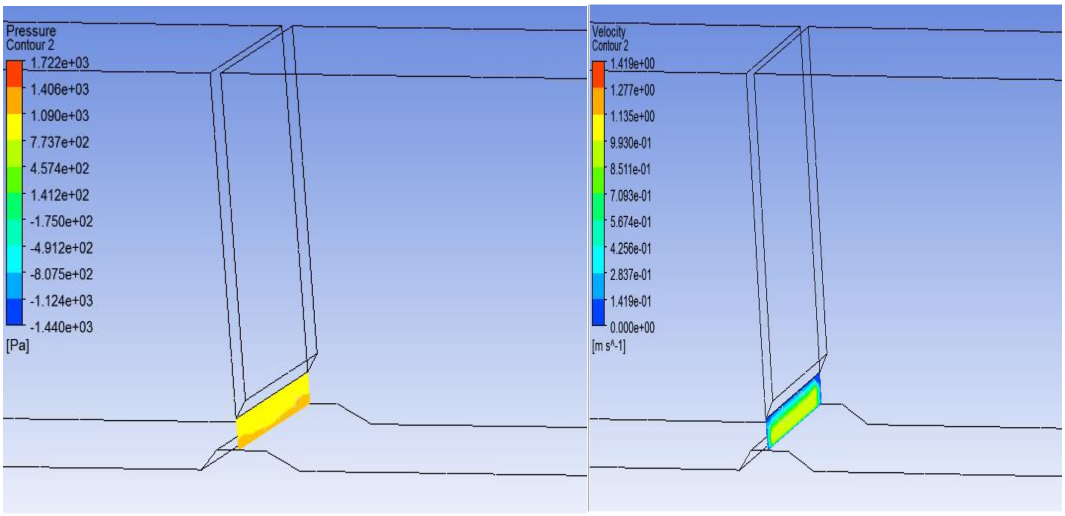

Figure 3. 10: Pressure variation and velocity variation just above the sill

(2) Upstream Depth is fixed at 0.10 m, and Sluice gate opening is fixed at G1

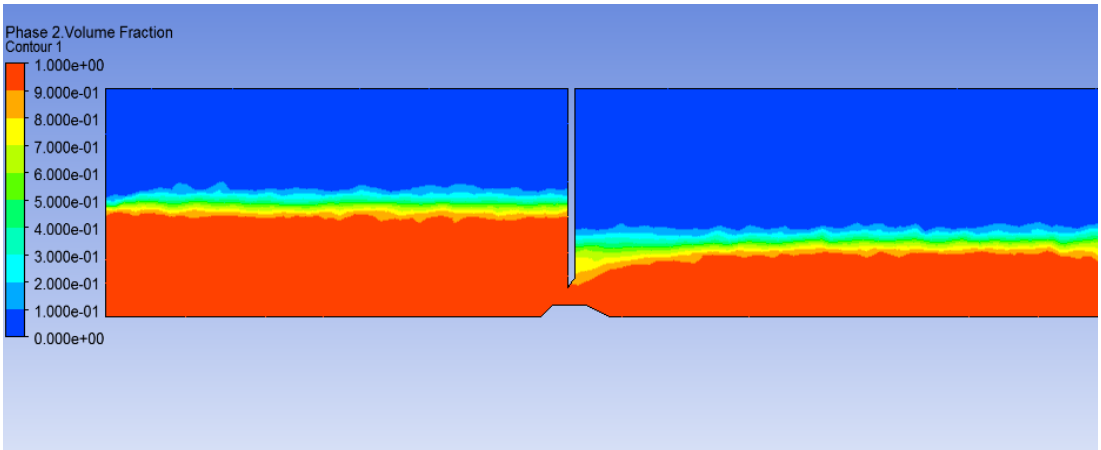

Figure 3. 11: Volume fraction Contour:

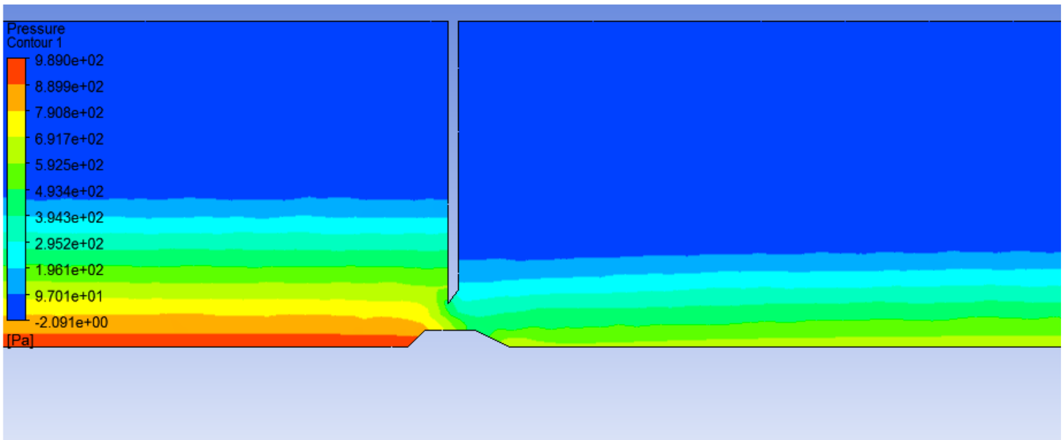

Figure 3. 12: Pressure Contour:

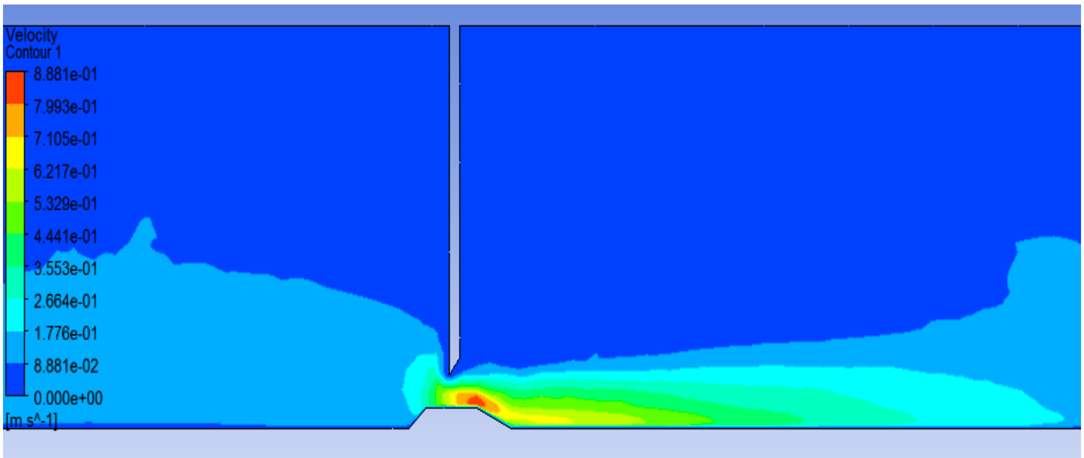

figure 3. 13: Velocity Contour

(3) Upstream Depth is fixed at 0.10 m, and Sluice gate opening is fixed at G2

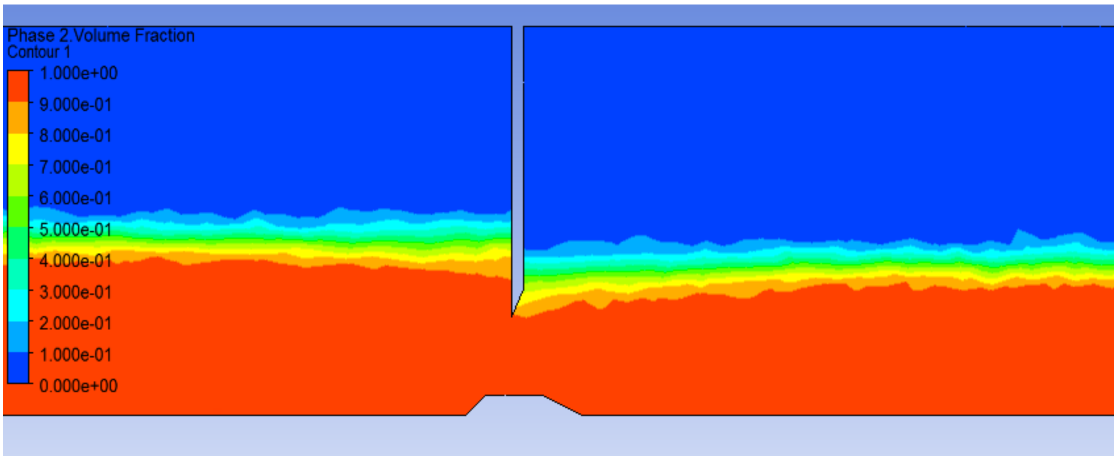

figure 3. 14:Volume fraction Contour

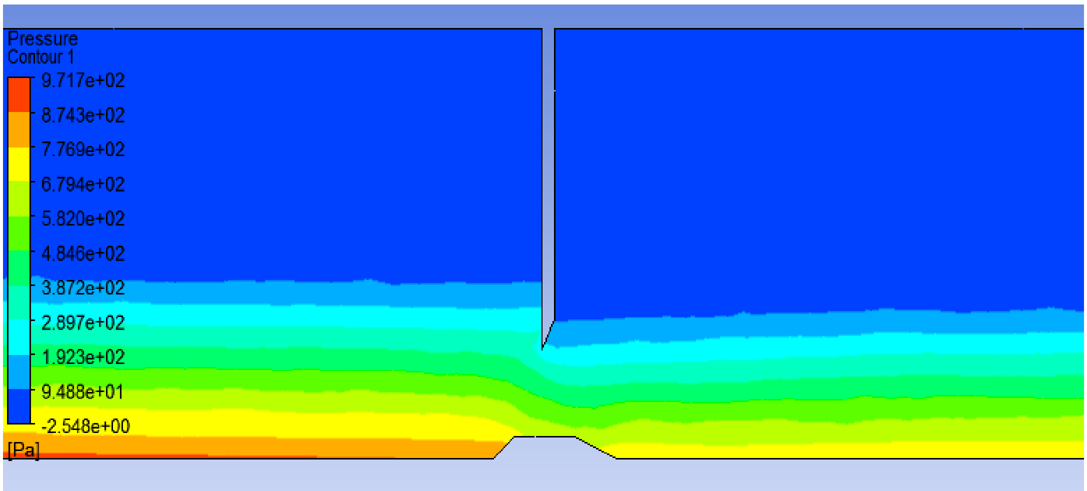

Figure 3.15 Pressure Contour:

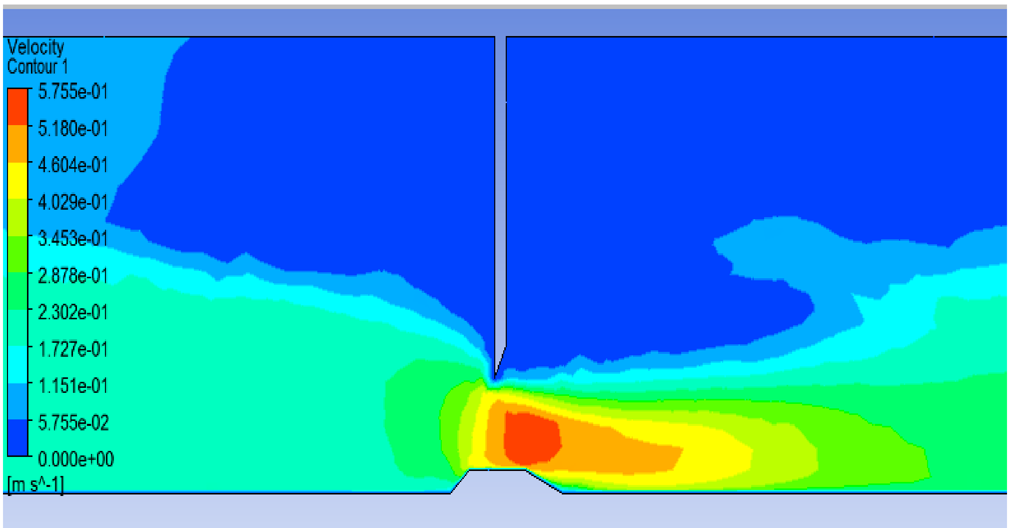

Figure 3.16 Velocity Contour

3.5.2 Model Type 2 (SILL HEIGHT Z=2 cm)

(a)Upstream Depth is fixed at 0.10 m, Sluice gate opening is fixed at G1

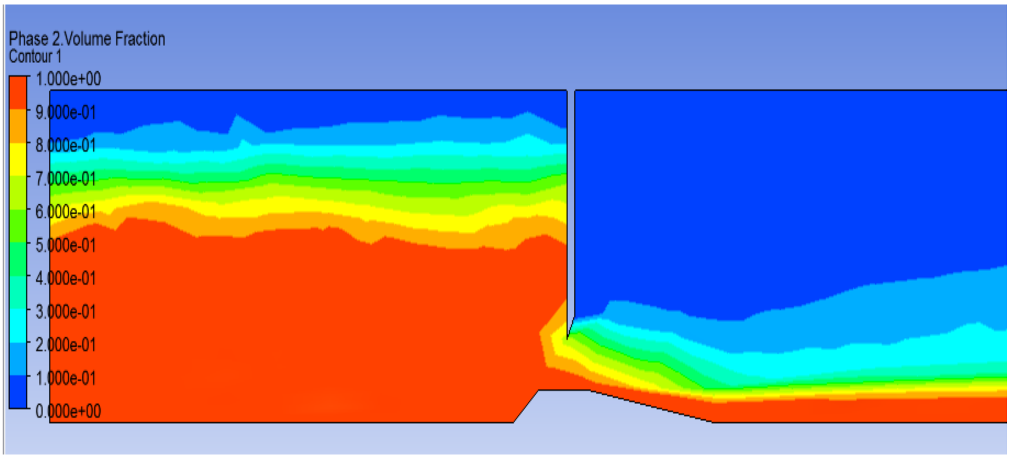

figure 3. 15 : Model type2 volume fraction Contours

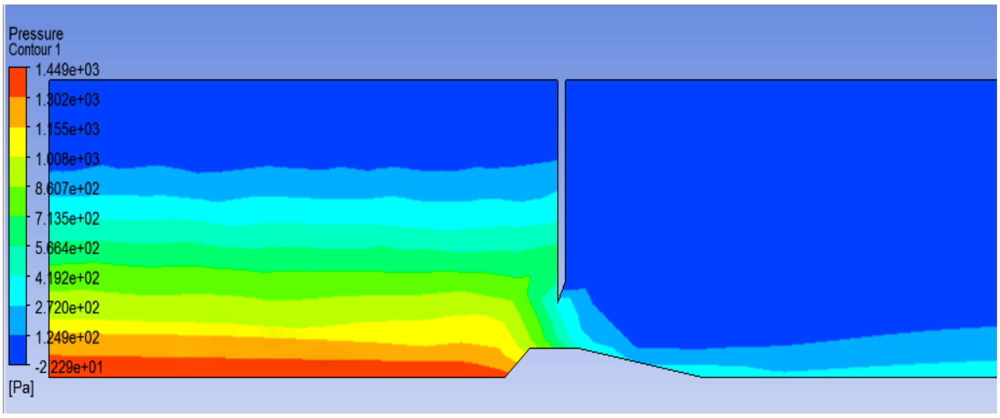

Figure 3.18 Pressure contour

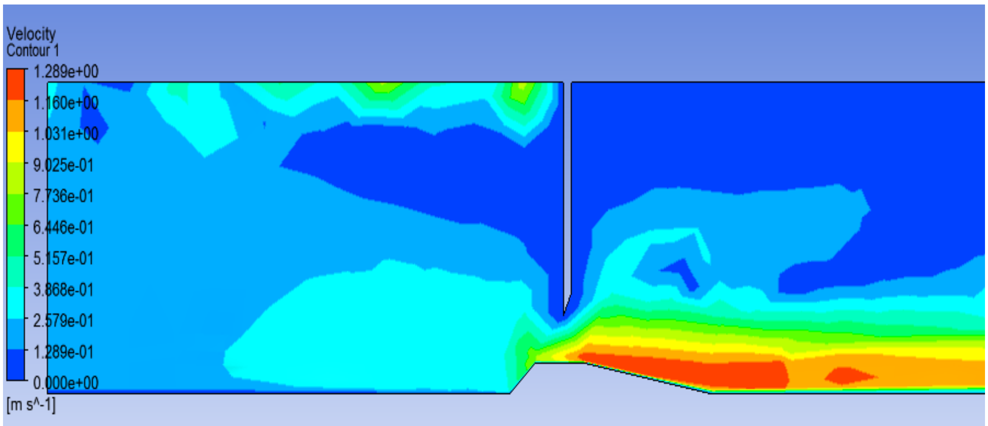

Figure 3.19 velocity contour

3.5.3 Model Type 3 (SILL HEIGHT Z=3 cm)

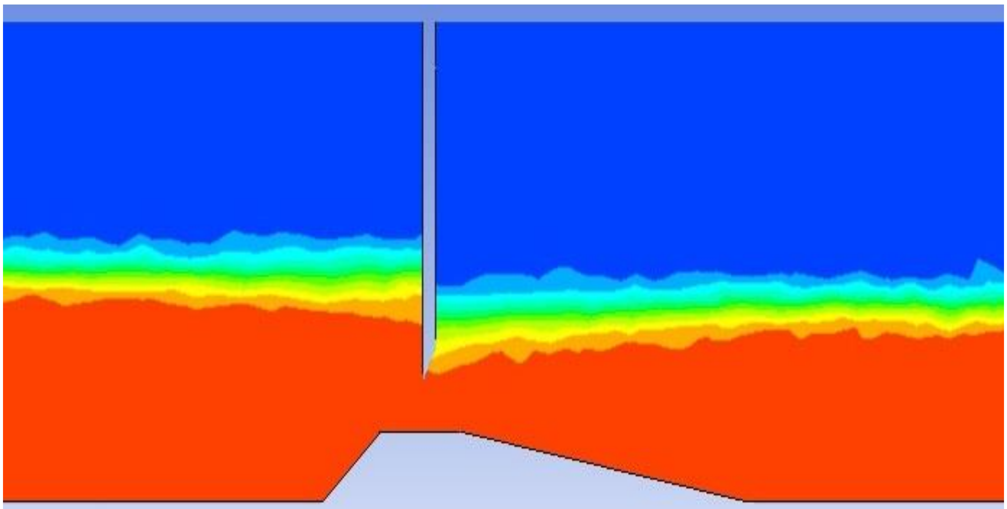

figure 3. 16 : Model type 3 volume fraction contour

3.5.4 Model Type 4 (SILL HEIGHT Z=4 cm)

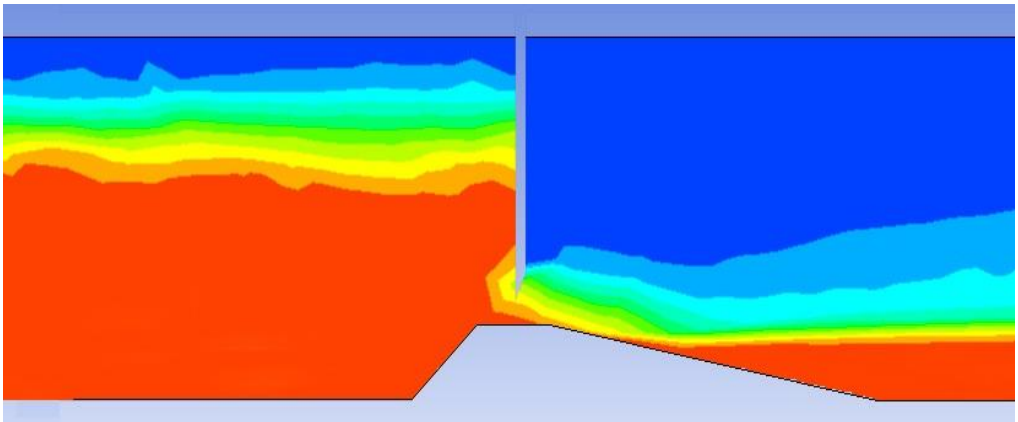

figure 3. 17: Model type4 volume fraction contour

Table 1: Subcritical flow z/b

z (cm)	**b (cm)**	**z/b**	**C_d**
1	3	0.3333	0.6541
2	3	0.6667	0.6560
3	3	1.0000	0.6526
4	3	1.3333	0.6600

Table 2:Subcritical flow ratio z/B

Z (cm)	**B (cm)**	**z/B**	**C_d**
1	9	0.1111	0.6531
2	15	0.1333	0.6541
3	21	0.1429	0.6543
4	27	0.1481	0.6629

Table 3:Supercritical flow z/b

Z (cm)	**B (cm)**	**z/b**	**C_d**
1	3	0.3333	0.6389
2	3	0.6667	0.6567
3	3	1.0000	0.6553
4	3	1.3333	0.6527

Table 4:Supercritical flow z/B

Z (cm)	**B (cm)**	**z/B**	**C_d**
1	9	0.1111	0.6389
2	15	0.1333	0.6567
3	21	0.1429	0.6553
4	27	0.1481	0.6527

Table 5:upstream depth H1/G

G (cm)	H1 (cm)	H1/G	Z=1cm	Z=2cm	Z=3cm	Z=4cm
3	8	2.67	0.6355	0.6541	0.6526	0.6526
3	10	3.33	0.6380	0.6550	0.6530	0.6500
3	11	3.67	0.6390	0.6558	0.6540	0.6527
3	13	4.33	0.6400	0.6590	0.6580	0.6533
3	15	5.00	0.6420	0.6600	0.6590	0.6550

3.6 GRAPHICAL PRESENTATIONS

(1) Plot between Coefficient of discharge and z/b.

(a) For Subcritical Flow

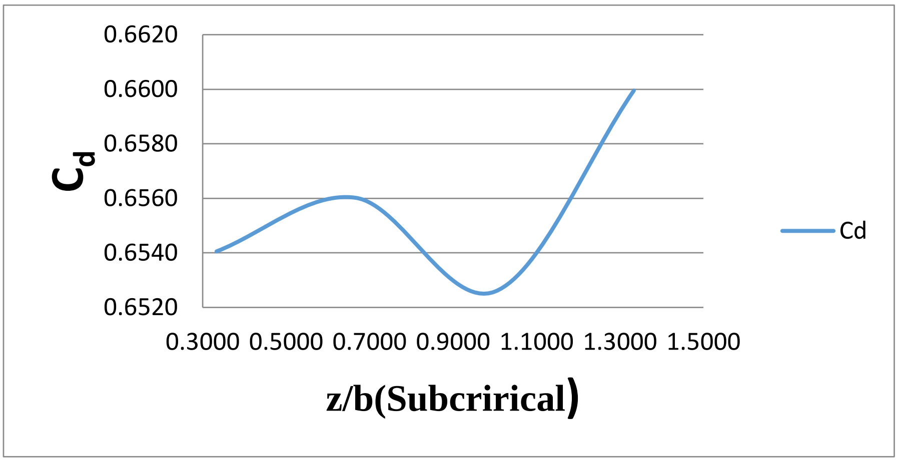

The average Cd tends to increase as the z/b value rises from 0 to 0.65, Then it declines until it reaches z/b=0.95., Then it quickly rises to z/b=1.3, implying that z/b has a substantial impact on the average coefficient discharge for subcritical flow (Fr 1). So according to previous research, Cd maximum levels were also found at z/b=1.0.

(b) Supercritical Flow

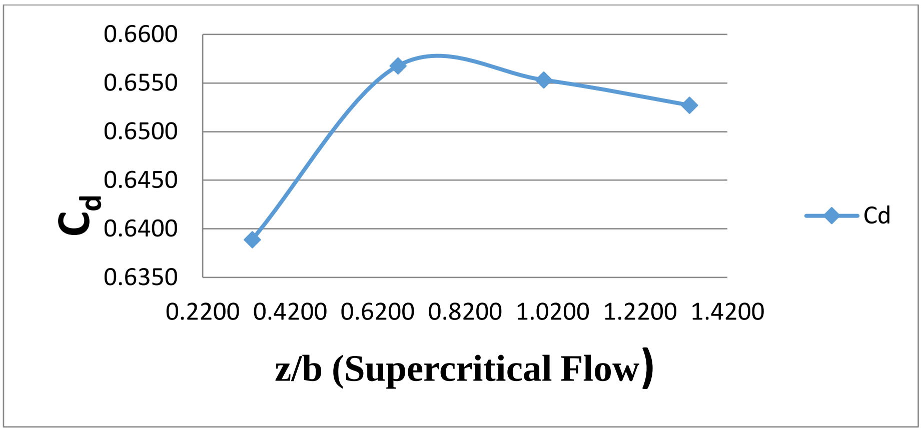

It is noticed that when z/b increases from 0 to 0.62, average C_d declines at a relatively slow pace, indicating that in the low Froude number range, supercritical flow is ($1 < F < 2$), the influence of z/b on the coefficient of discharge is small.

(2) Plot between Coefficient of discharge and z/B.

(a) For Subcritical Flow

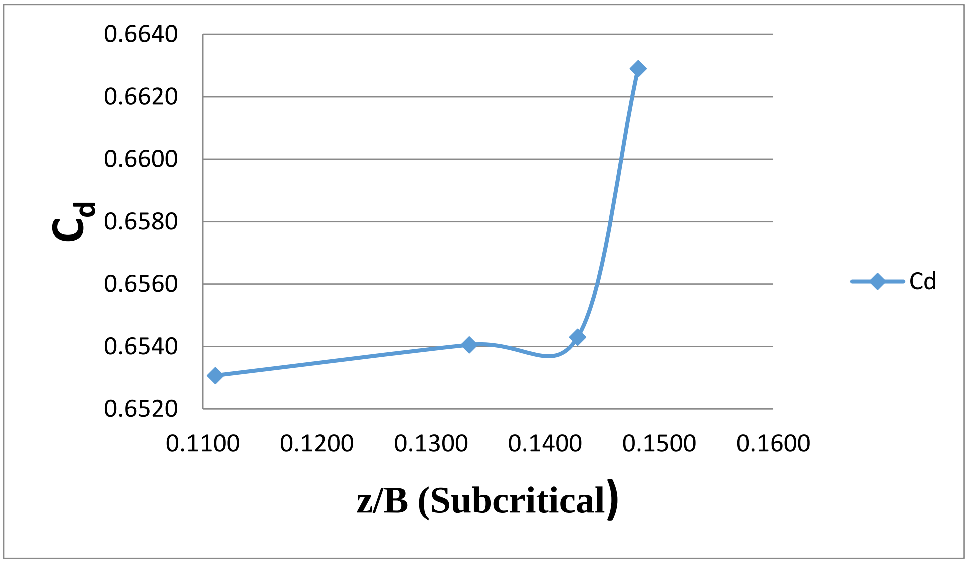

The average value of Cd, on the other hand, rises with increasing z/B from 0 to 0.135, then falls a little until z/B=0.142. Then it rises quickly to z/B=0.148, showing that z/B=0.135 is the maximum value for submerged subcritical flow.

(b) For Supercritical Flow

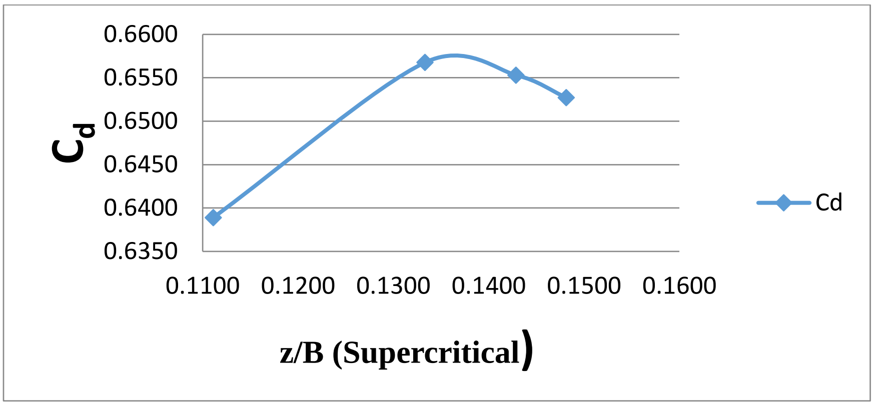

The average value of Cd, on the other hand, rises with the rises in z/B from 0.05 to 0.14 and then falls a little beyond z/B=0.14, showing that maximum levels of Cd are obtained for supercritical flow at a low Froude number at z/B=0.14.

(3) Variation of Coefficient of discharge for a fixed gate opening and varying upstream head.

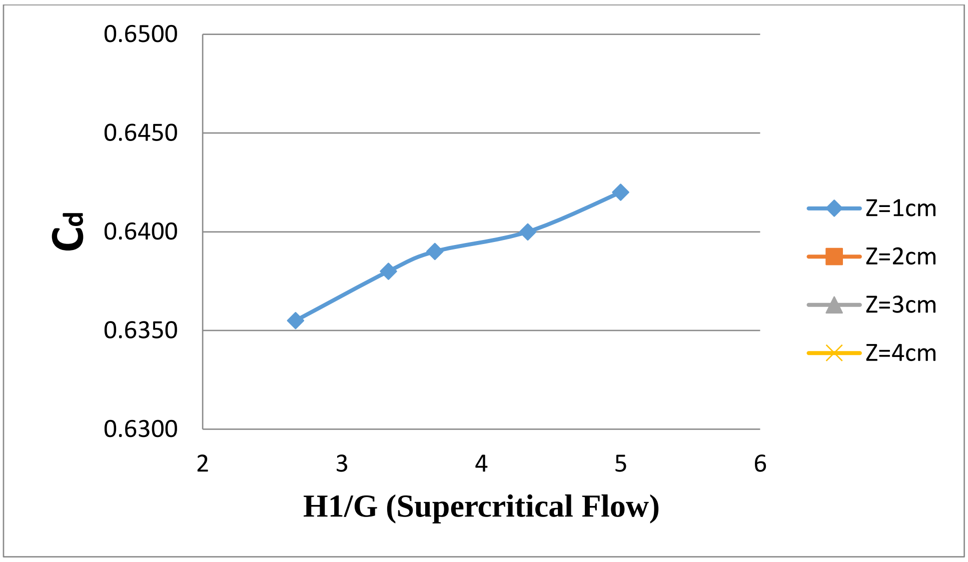

The trend of Cd fluctuation with H1/ G decreases rapidly as H1/ G grows. Changes in z/B and z/b cause variations in the above figure at constant H1/G. Similar to the supercritical flow regime, higher z/B, and z/b values result in higher Cd.

CHAPTER 4:
CONCLUSION AND DISCUSSIONS

The following results are obtained from the analysis of CFD simulations using Ansys fluent software relating the result to the experimental research papers which have been done earlier.

1) Based on simulation results, submerged flow properties are presented and discussed. ΔH/G which is the head-gate opening ratio difference, H1/G the upstream head-gate opening ratio, and z/b, Z/B the sill parameter all influence the coefficient of discharge.
2) It was discovered that for submerged subcritical flow, the rate at which the discharge coefficient changes are higher and moderate for the critical submerged flow, and for submerged supercritical flow the rate of change of the coefficient discharge is mostly constant.
3) The discharge coefficient ranges between 0.63-0.66 which confirms the past studies and the trend of the present work are almost similar to the previously published work so this work may be reliable.
4) In comparison to other downstream slopes of sills, studies have shown that the trapezoidal sill with a downstream slope of 1V:5H enhances discharge below the gate and generates the lowest increase in the jump length formed downstream. Trapezoidal sill is also economical as reducing the material cost.
5) Higher Z/b or Z/B results in higher discharge coefficients, according to the findings. The values due to no-sill, Z/b =Z/B =0.0, on the other hand, are the smallest.
6) The average Cd tends to increase as the z/b value rises from 0 to 0.65, Then it declines until it reaches z/b=0.95., Then it quickly rises to z/b=1.3, implying that z/b has a substantial impact on the average coefficient discharge for subcritical flow (Fr 1). So according to previous research, Cd maximum levels were also found at z/b=1.0.
7) The discharge coefficient slightly increases as the height of sill (Z) increases.

8) In Ansys fluent Analysis trends between dimensionless parameters are plotted graphically and compared with the previous study done by researchers which is most reliable.
9) The prismatic sills beneath the sluice gate improve free flow effectiveness due to the lowered head generated in front of the gate for certain discharges. The gradual inlet and outlet of the sill slopes affect the curvature of streamlines, resulting in this reduction.
10) The prismatic sills beneath the sluice gate improve free flow performance by up to 25% as conclusion by previous research experiments.
11) Previous experimental researches shows that higher the sill under the gate, the lower the backup water depth and submerged jump length, but the higher the energy loss. As the sill height rises, both forward and reverse flow rises.
12) The near-bed velocity is maximum when the sill under the gate is significantly greater.
13) With increasing (P/d, H/d, and P/W), the coefficient of discharge rises.

REFERENCE

[1] W. I. T. Press, "Transactions on Modelling and Simulation vol 10, © 1995 WIT Press, www.witpress.com, ISSN 1743-355X," vol. 10, 1995.

[2] H. Ali and A. Elhamaimi, "An Experimental and Numerical Investigation for Characteristics of Submerged Hydraulic Jump over Corrugated Beds," Port-Said Eng. Res. J., vol. 0, no. 0, pp. 0–0, 2020, doi: 10.21608/pserj.2020.18744.1015.

[3] N. Afzal, A. Bushra, and A. Seena, "Analysis of Turbulent Hydraulic Jump over a Transitional Rough Bed of a Rectangular Channel : Universal Relations Analysis of Turbulent Hydraulic Jump over a Transitional Rough Bed of a Rectangular Channel : Universal Relations," no. October 2016, 2011, doi: 10.1061/(ASCE)EM.

[4] S. Jaiswal and B. Jhamnani, "CFD Analysis Of Non-Prismatic Compound Channel," Int. J. Mod. Trends Eng. Res., vol. 5, no. 7, pp. 122–129, 2018, doi: 10.21884/ijmter.2018.5187.0byxj.

[5] A. Mohanta, K. C. Patra, and K. K. Khatua, "OPEN ACCESS CFD Simulation And Two-Phase Modeling Of A Non-Prismatic Converging Compound Channel," no. March, pp. 17–23, 2014.

[6] S. Sunik, "Characteristic of Contraction," J. Tek. Sipil, vol. 15, no. 3, pp. 170–175, 2019.

[7] A. A. Alhamid, "Coefficient of Discharge for Free Flow Sluice Gates," J. King Saud Univ. - Eng. Sci., vol. 11, no. 1, pp. 33–47, 1999, doi: 10.1016/S1018-3639(18)30989-9.

[8] A. Yıldız, "COMPARISON OF EXPERIMENTAL STUDY AND CFD ANALYSIS OF THE FLOW UNDER A SLUICE GATE," pp. 251–255, 2015.

[9] N. AboulAtta, G. Ezizah, N. Yousif, and S. Fathy, "Design of stilling basins using artificial roughness," World Acad. Sci. Eng. Technol., vol. 74, no. January 2021, pp. 1–7, 2011.

[10] E. A. Elnikhely, "Discharge Characteristics Through Vertical Sluice Gate in a Sudden Expanding Stilling Basin," vol. 11, no. 5, pp. 585–599, 2020.

[11] M. Debabeche and B. Achour, "Effect of sill in the hydraulic jump in a triangular channel/ Effet du seuil sur le ressaut hydraulique dans un canal triangulaire," J. Hydraul. Res., vol. 45, no. 1, pp. 135–139, 2007, doi:

10.1080/00221686.2007.9521753.

[12] M. Ghodsian, “Flow-through Side Sluice Gate,” J. Irrig. Drain. Eng., vol. 129, no. 6, pp. 458–463, 2003, doi: 10.1061/(asce)0733-9437(2003)129:6(458).

[13] A. Mohanta, B. Naik, K. C. Patra, and K. K. Khatua, “Experimental and Numerical Study of Flow in Prismatic and Non-prismatic Section of a Converging Compound Channel,” vol. 5, no. 3, pp. 203–210, 2014.

[14] D. Lozano, L. Mateos, G. P. Merkley, and A. J. Clemmens, “Field Calibration of Submerged Sluice Gates in Irrigation Canals,” J. Irrig. Drain. Eng., vol. 135, no. 6, pp. 763–772, 2009, doi: 10.1061/(asce)ir.1943-4774.0000085.

[15] M. Esmailzadeh, M. Heidarpour, and S. S. Eslamian, “Flow Characteristics of a Sharp-Crested Side Sluice Gate,” pp. 1–6, doi: 10.1061/(ASCE)IR.1943-4774.0000852.

[16] E. Kubrak, J. Kubrak, A. Kiczko, and M. Kubrak, “Flow measurements using a sluice gate; Analysis of applicability,” Water (Switzerland), vol. 12, no. 3, 2020, doi: 10.3390/w12030819.

[17] “ª ¬ ’ G ’ Z ’,” vol. 5, no. 3, p. 2011, 2011.

[18] T. Boeckmann, Y. Bozhko, A. Tukimin, M. Zuber, and K. A. Ahmad, “Estimation Optimal Value of Discharge Coefficient in a Venturi Tubes Estimation Optimal Value of Discharge Coefficient in a Venturi Tubes,” 2019, doi: 10.1088/1742-6596/1230/1/012087.

[19] P. Taylor, J. F. Yen, C. H. Lin, C. T. Tsai, and C. Lin, “Journal of the Chinese Institute of Engineers Hydraulic characteristics and discharge control of sluice gates,” no. November 2014, pp. 37–41, doi: 10.1080/02533839.2001.9670628.

[20] S. A. Ead and N. Rajaratnam, “Hydraulic Jumps on Corrugated Beds,” no. July, pp. 656–663, 2002.

[21] S. Jalil and S. A. Sarhan, “Hydraulic Jump Properties Downstream a Sluice Gate with Prismatic Sill Hydraulic Jump Properties Downstream a Sluice Gate with Prismatic Sill,” no. April, 2019, doi: 10.19026/rjaset.11.1801.

[22] E. Demirel, “Measured and simulated flow downstream of the submerged sluice gate,” Water Environ. J., vol. 29, no. 3, pp. 446–455, 2015, doi: 10.1111/wej.12119.

[23] M. C. Aydın and A. E. Ulu, “Numerical modeling of sluice gates with different sill types under submerged flow conditions,” Bitlis Eren Univ. J. Sci. Technol., vol. 7, no. 1, pp. 1–1, 2017, doi: 10.17678/beuscitech.310157.

[24] D.-G. Kim, "Numerical analysis of free flow past a sluice gate," KSCE J. Civ. Eng., vol. 11, no. 2, pp. 127–132, 2007, doi: 10.1007/bf02823856.

[25] S. Al Hashimi, "Space with a font size 24 Space with a font size 24," no. May 2018, 2019.

[26] F. Salmasi and J. Abraham, "geometric sills under the gate using multiple non-linear regression (MNLR)," J. Hydrol., p. 125728, 2020, doi: 10.1016/j.jhydrol.2020.125728.

[27] A. Habibzadeh, S. M. Asce, A. R. Vatankhah, N. Rajaratnam, and F. Asce, "Role of Energy Loss on Discharge Characteristics of Sluice Gates," no. SEPTEMBER, pp. 1079–1084, 2011, doi: 10.1061/(ASCE)HY.

[28] S. Karami, M. Mehdi, H. Mohammad, and H. Adib, "Investigation of Free Flow Under the Sluice Gate with the Sill Using Flow - 3D Model," Iran. J. Sci. Technol. Trans. Civ. Eng., no. 1950, 2019, doi: 10.1007/s40996-019-00310-x.

[29] P. K. Swamee, "Sluice-Gate Discharge Equations," J. Irrig. Drain. Eng., vol. 118, no. 1, pp. 56–60, 1992, doi: 10.1061/(asce)0733-9437(1992)118:1(56).

[30] C. M. Burt and A. J. Clemmens, "Flow Rate Equation for Suppressed and Submerged Sluice Gates Prepared by," vol. 001, no. 805, 2020.

[31] A. M. Negm and A. A. Alhamid, "Submerged Flow Below Sluice Gate With Sill," no. February 2014, 1998.

[32] S. Jalil, "Submerged Flow Analysis below a Vertical Gate with Stepped Sill Caspian Journal of Applied Sciences Research Submerged Flow Analysis below a Vertical Gate with Stepped Sill," no. April, 2017.

[33] S. Jalil, S. Sarhan, and S. Ibrahim, "Effect of Prismatic Sill on the Performance of Free Flow under Sluice Gate," Sci. J. Univ. Zakho, vol. 4, no. 1, pp. 150–158, 2016, doi: 10.25271/2016.4.1.353.